Like DNA Replication, Eukaryotic DNA Mismatch Repair is Asymmetric

June 19th 2012

Sascha Emilie Liberti
DNA replication fidelity group
NIEHS

Polymerase Mutator Alleles – The Toolset

	Motif A		Family B
S.cer α	863	MDFNSLYPSIIQEFN	877
S.cer δ	607	LDFNSLYPSIMMAHN	621
S.cer ε	639	VDVASMYPNIMTTNR	653

Pol α L868M

Pol δ L612M

Pol ε M644G

Strand-Specific Error Signature

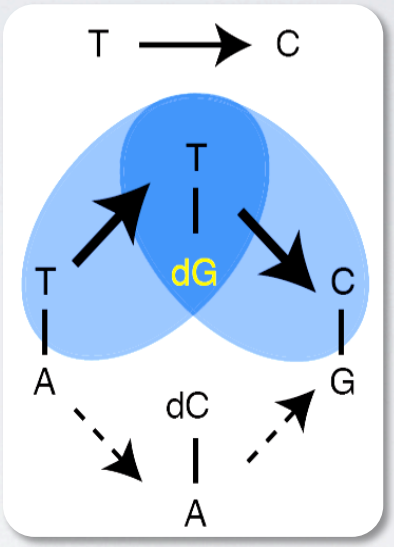

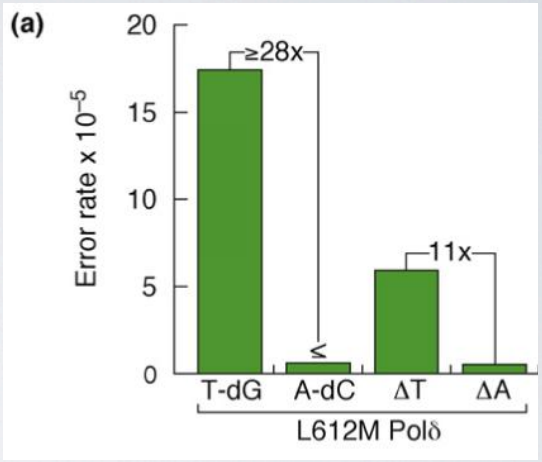

Kunkel and Burgers 2008

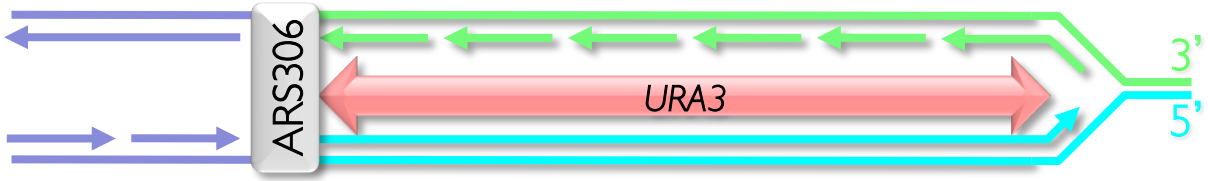

Division of Labor at the Eukaryotic Replication Fork

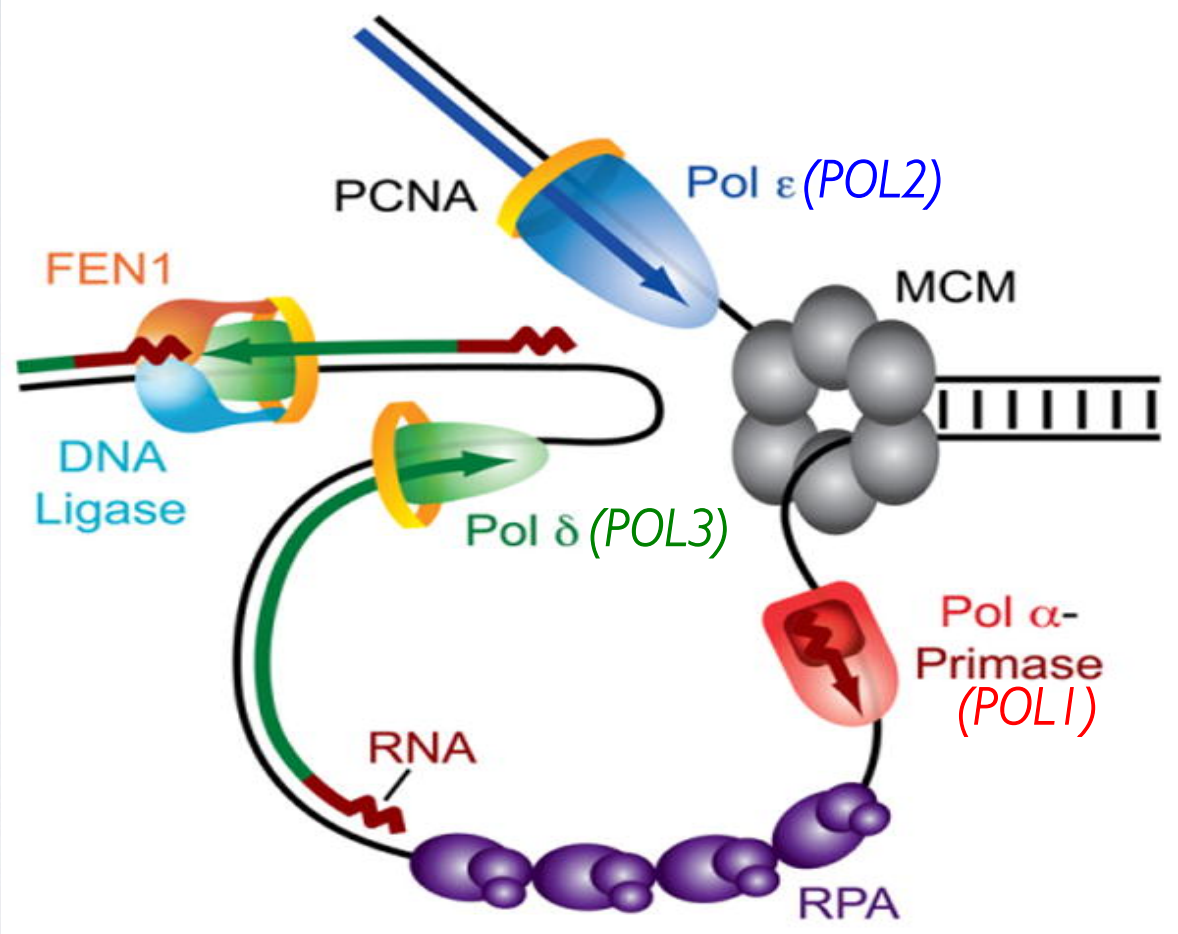

Pursell et al. (2007)
Nick McElhinny et al. (2008)
Kunkel & Burgers (2008)
Larrea et al. PNAS (2010)

DNA mismatch repair

Replication error

Mismatch recognition

MMR complex assembly
and
Strand discrimination

Excision

Re-synthesis

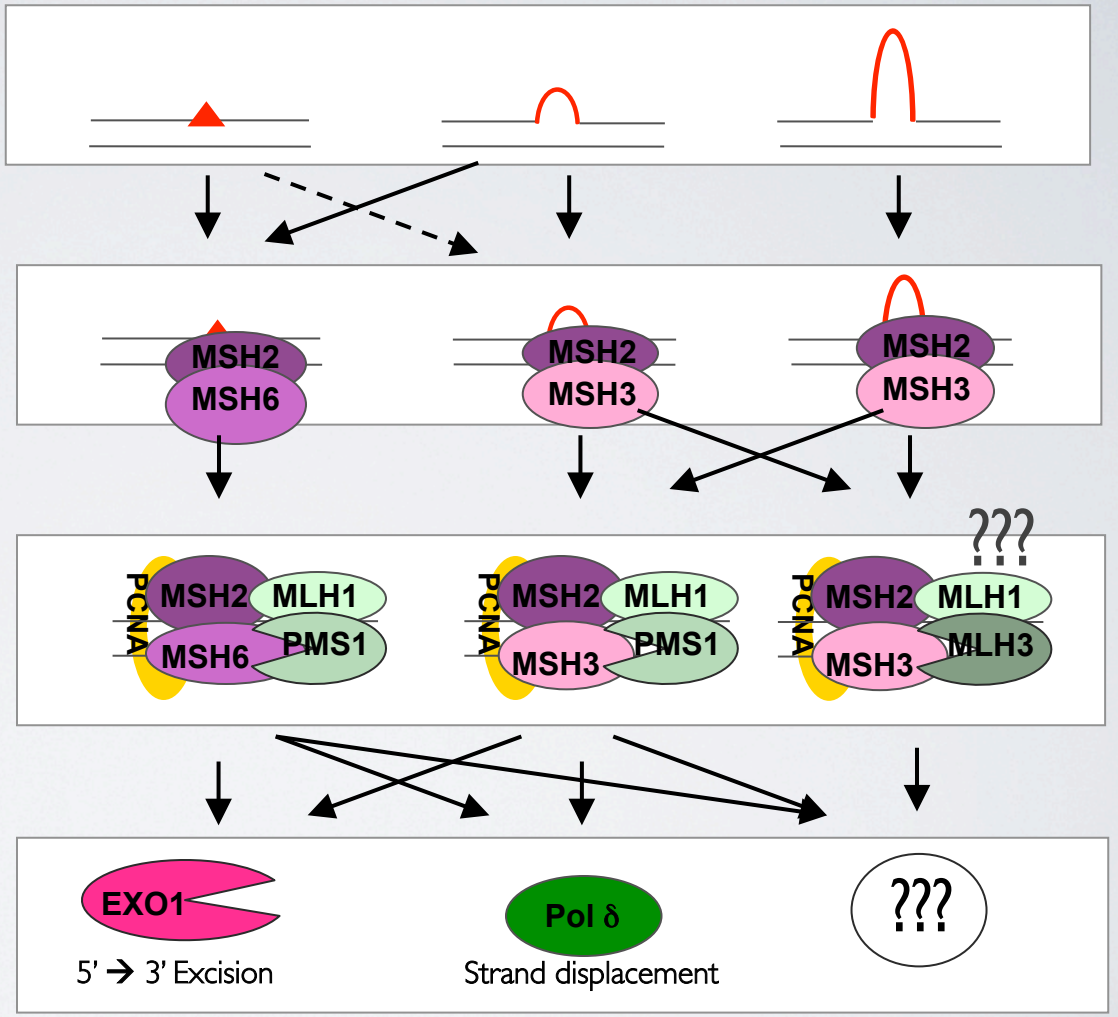

MMR more efficiently repairs errors introduced by pol α than pol δ

Nick McElhinny et. al. PNAS 2010

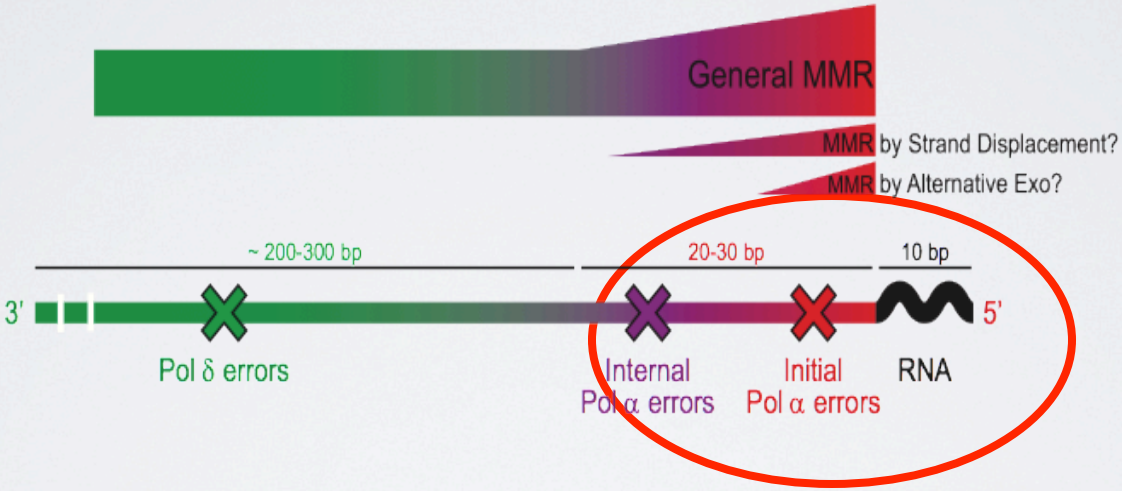

Working hypothesis

Is Exo1 involved in the higher MMR efficiency observed for pol α errors?

Mutation rates in *exo1Δ* strains

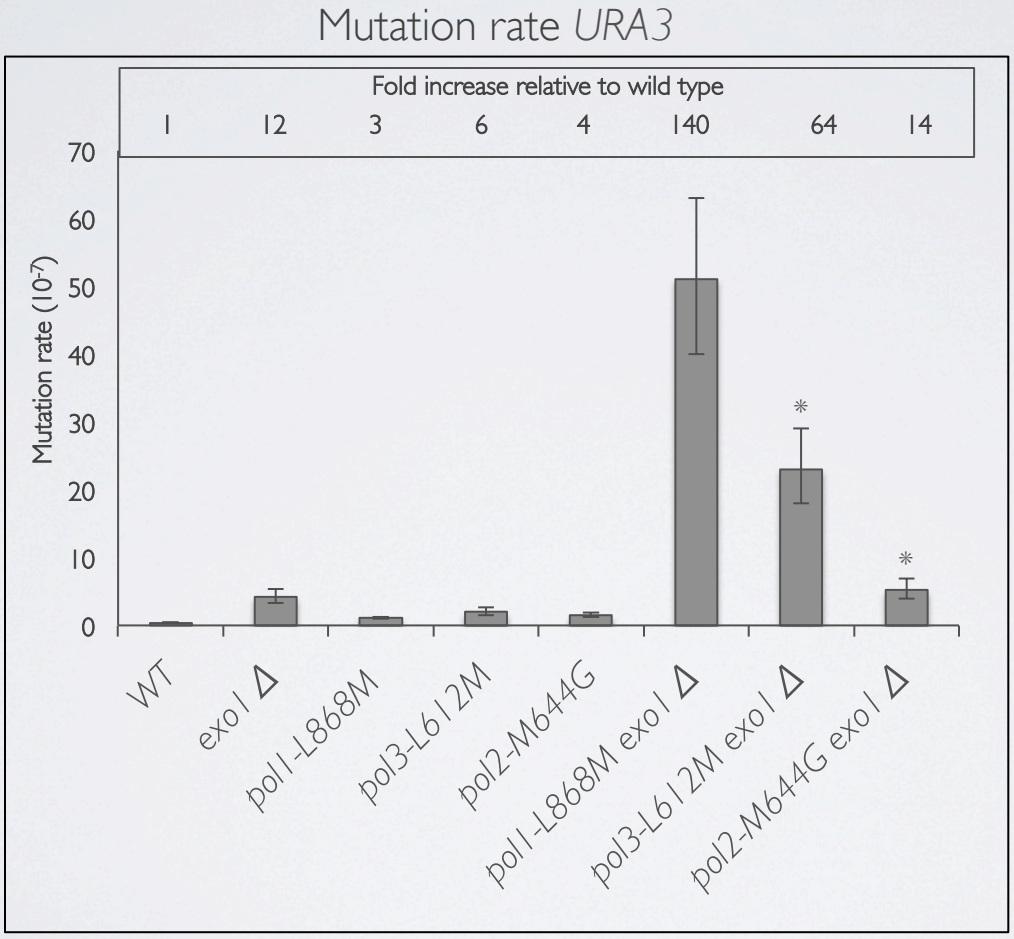

* Hombauer et al., 2011 *Cell*

Mutation rates in *exo1Δ* strains

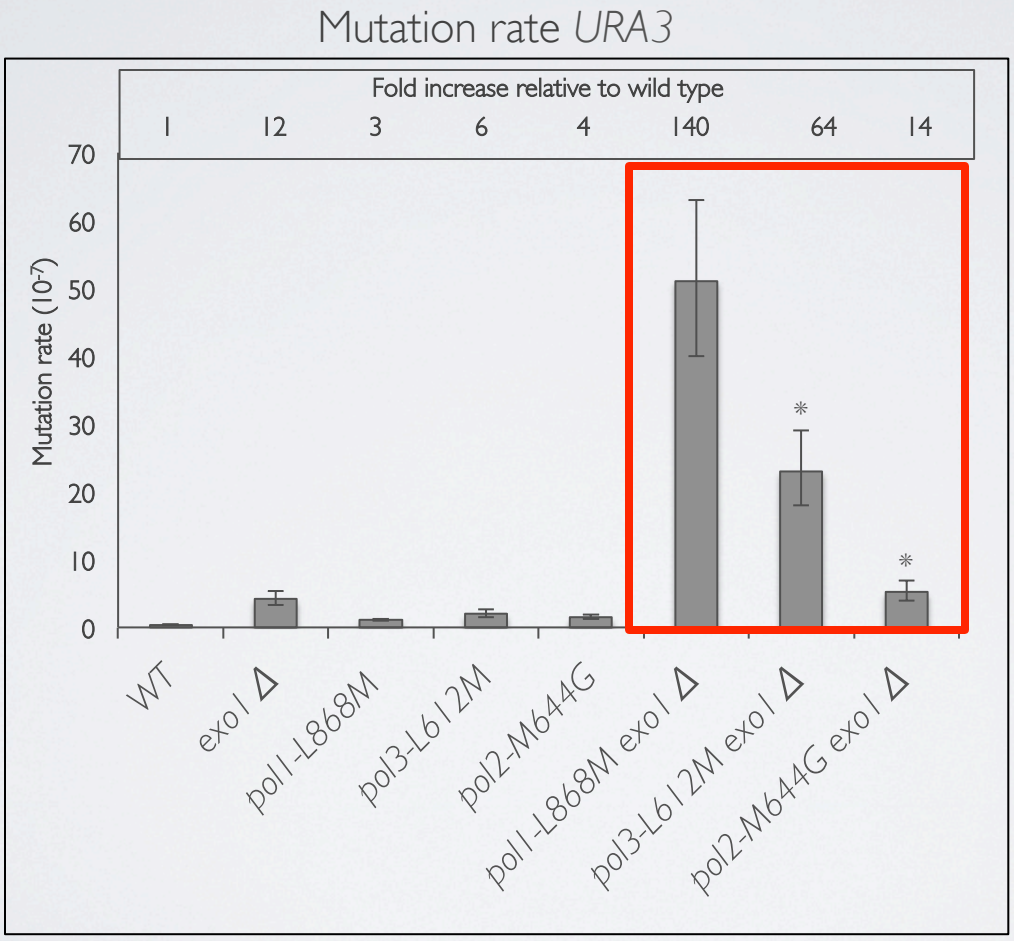

Exo1 dependent increase in mutation rate
pol **α** > pol **δ** > pol **ε**

* Hombauer et al., 2011 *Cell*

Mutation rates in *exo1Δ* strains

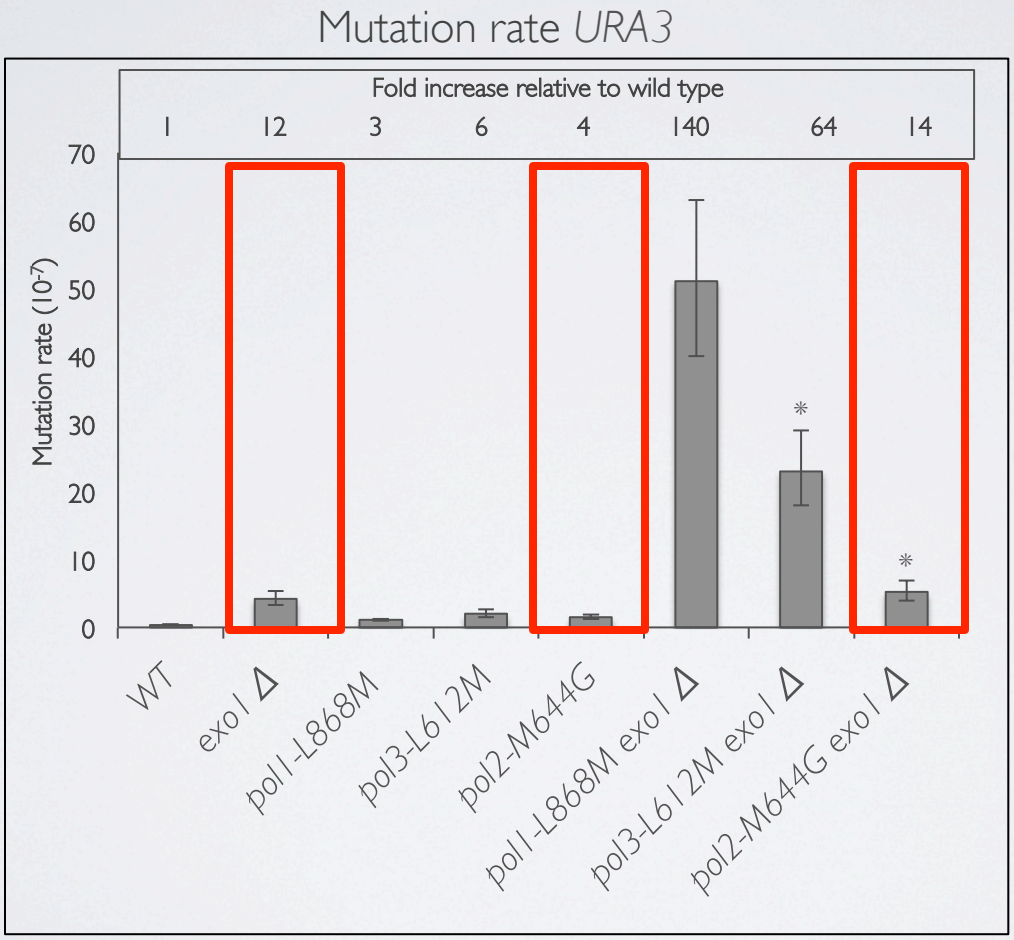

Little involvement of Exo1 in repair of pol **ε** errors

* Hombauer et al., 2011 *Cell*

Mutations in *exo1*Δ strains are base substitutions and single base deletions

Indicative of MMR loss

Mutation Specificity in *pol1-L868M exo1Δ and pol3-L612M exo1Δ* strains

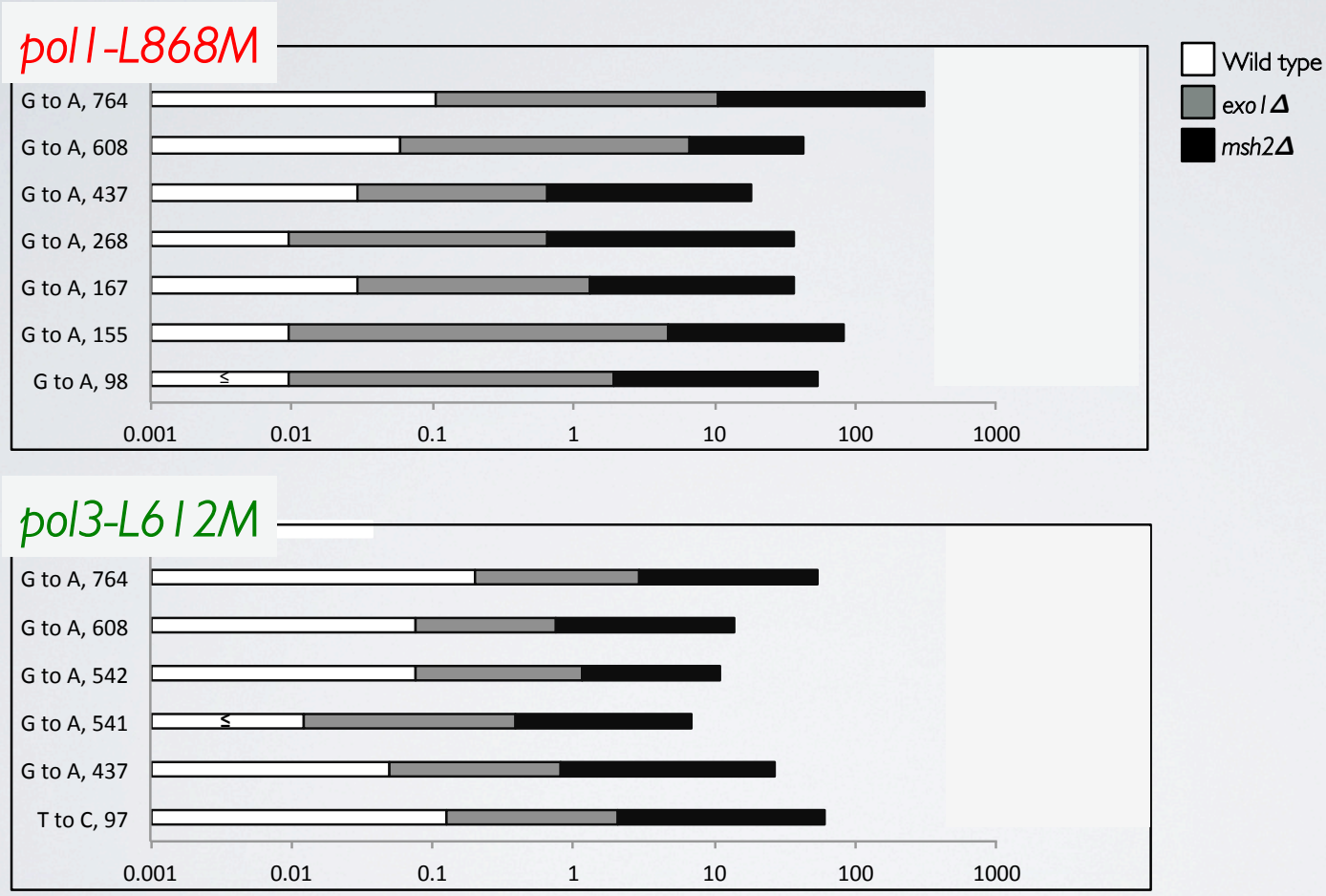

Wild type and Msh2 data are from:
Nick McElhinny et. al. PNAS 2010

Mutation Specificity in *pol1-L868M exo1Δ and pol3-L612M exo1Δ* strains

pol1-L868M

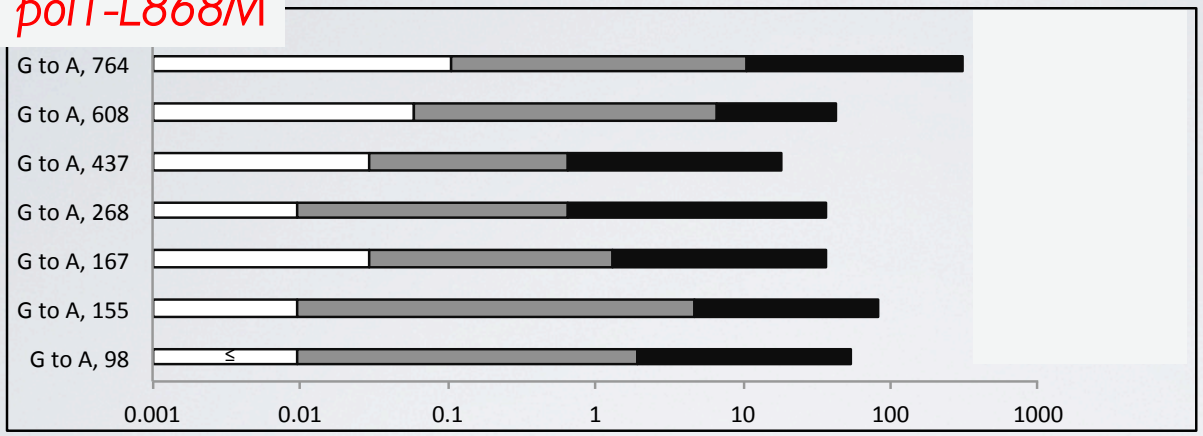

Correction factor:

$$\frac{exo1\Delta}{EXO1^{+}}$$

pol3-L612M

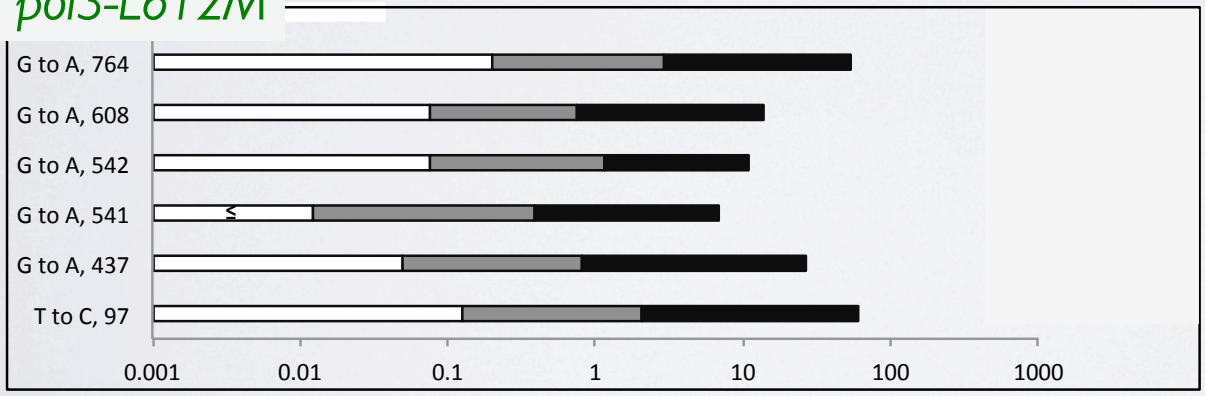

Wild type and Msh2 data are from:
Nick McElhinny et. al. PNAS 2010

Mutation Specificity in *pol1-L868M exo1Δ and pol3-L612M exo1Δ* strains

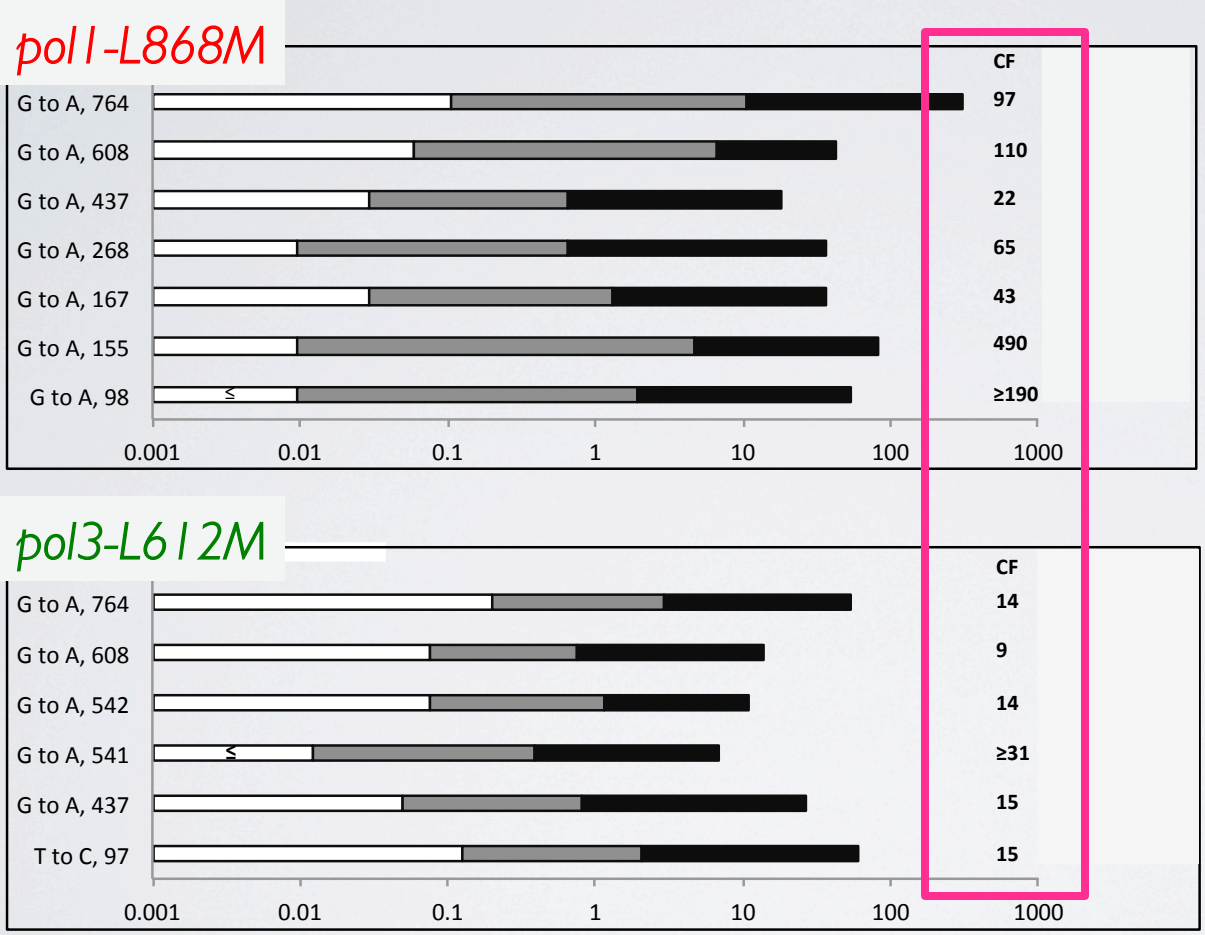

Wild type
exo1Δ
msh2Δ

Correction factor:

$$\frac{exo1\Delta}{EXO1^{+}}$$

Wild type and Msh2 data are from:
Nick McElhinny et. al. PNAS 2010

Mutation Specificity in *pol1-L868M exo1Δ and pol3-L612M exo1Δ* strains

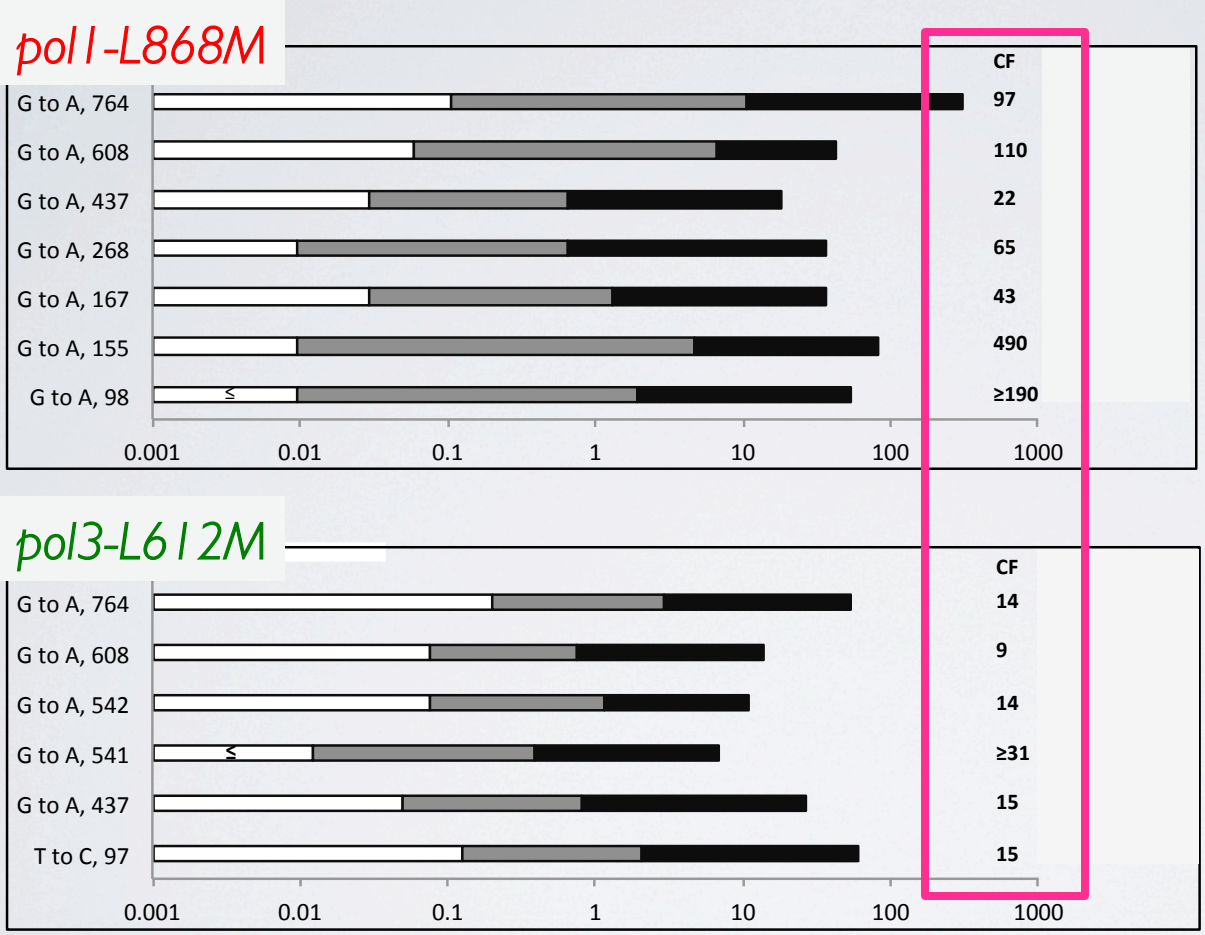

Exo1 repairs replication errors introduced by pol **α** more efficiently compared to errors introduced by pol **δ**

Wild type and Msh2 data are from:
Nick McElhinny et. al. PNAS 2010

Exo1 dependent mismatch repair of transitions

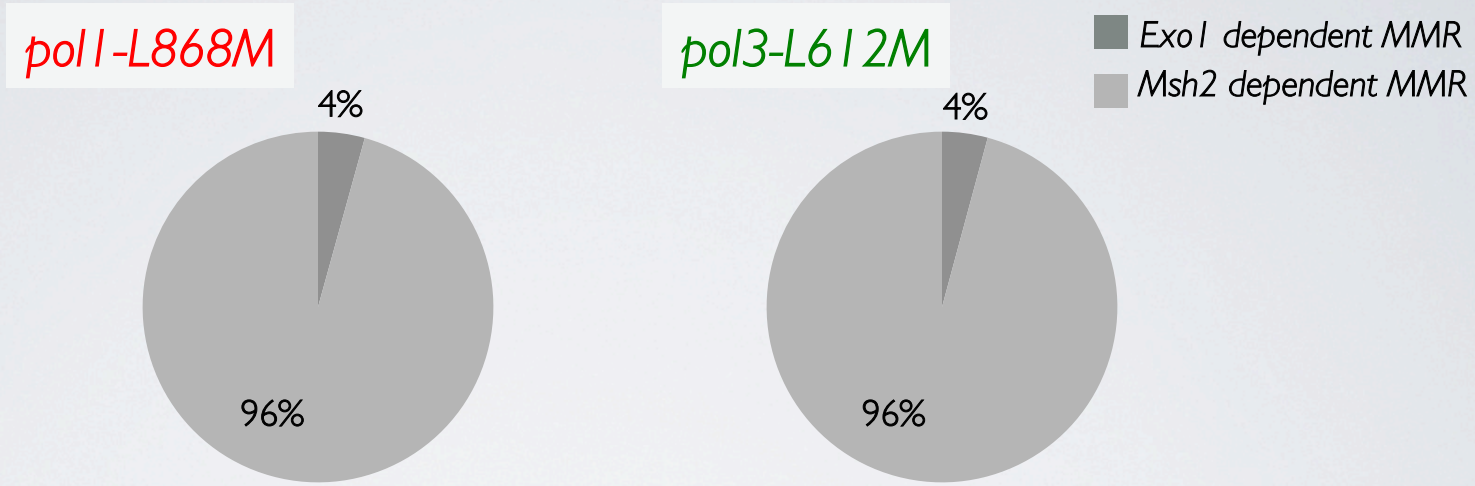

In the absence of Exo1 most replication errors can still be corrected through Msh2-dependent mechanisms

Msh2 data are from:
Nick McElhinny et. al. PNAS 2010

MMR deficient strains (*msh2Δ*) are characterized by very high single base deletion rates at four specific mononucleotide runs in *URA3*

Four mononucleotide runs in *URA3* are highly dependent on MMR

Specific rate at hotspot at 627 ΔG		Relative increase
Pol3LM	0.012	1
Pol3LM msh2Δ	16	1300
Pol3LM exo1Δ	0.1	8

Specific rate at hotspot at 605 ΔC		Relative increase
Pol3LM	0.012	1
Pol3LM msh2Δ	13	1000
Pol3LM exo1Δ	0.1	8

Specific rate at hotspot at 255 ΔT		Relative increase
Pol3LM	0.012	1
Pol3LM msh2Δ	90	7200
Pol3LM exo1Δ	0.1	8

Specific rate at hotspot at 201 ΔT		Relative increase
Pol3LM	0.012	1
Pol3LM msh2Δ	80	6500
Pol3LM exo1Δ	0.38	31

Wild type and Msh2 data are from:
Nick McElhinny et. al. PNAS 2010

Four mononucleotide runs in *URA3* are highly dependent on MMR

Specific rate at hotspot at 627 ΔG		Relative increase
Pol3LM	0.012	1
Pol3LM msh2Δ	16	1300
Pol3LM exo1Δ	0.1	8

Specific rate at hotspot at 605 ΔC		Relative increase
Pol3LM	0.012	1
Pol3LM msh2Δ	13	1000
Pol3LM exo1Δ	0.1	8

Specific rate at hotspot at 255 ΔT		Relative increase
Pol3LM	0.012	1
Pol3LM msh2Δ	90	7200
Pol3LM exo1Δ	0.1	8

Specific rate at hotspot at 201 ΔT		Relative increase
Pol3LM	0.012	1
Pol3LM msh2Δ	80	6500
Pol3LM exo1Δ	0.38	31

Wild type and Msh2 data are from:
Nick McElhinny et. al. PNAS 2010

Four mononucleotide runs in *URA3* are highly dependent on MMR – *But not on Exo1*

Specific rate at hotspot at 627 ΔG		Relative increase
Pol3LM	0.012	1
Pol3LM msh2Δ	16	1300
Pol3LM exo1Δ	0.1	8

Specific rate at hotspot at 605 ΔC		Relative increase
Pol3LM	0.012	1
Pol3LM msh2Δ	13	1000
Pol3LM exo1Δ	0.1	8

Specific rate at hotspot at 255 ΔT		Relative increase
Pol3LM	0.012	1
Pol3LM msh2Δ	90	7200
Pol3LM exo1Δ	0.1	8

Specific rate at hotspot at 201 ΔT		Relative increase
Pol3LM	0.012	1
Pol3LM msh2Δ	80	6500
Pol3LM exo1Δ	0.38	31

Wild type and Msh2 data are from:
Nick McElhinny et. al. PNAS 2010

Dissection of Exo1's functions in MMR sub-pathways

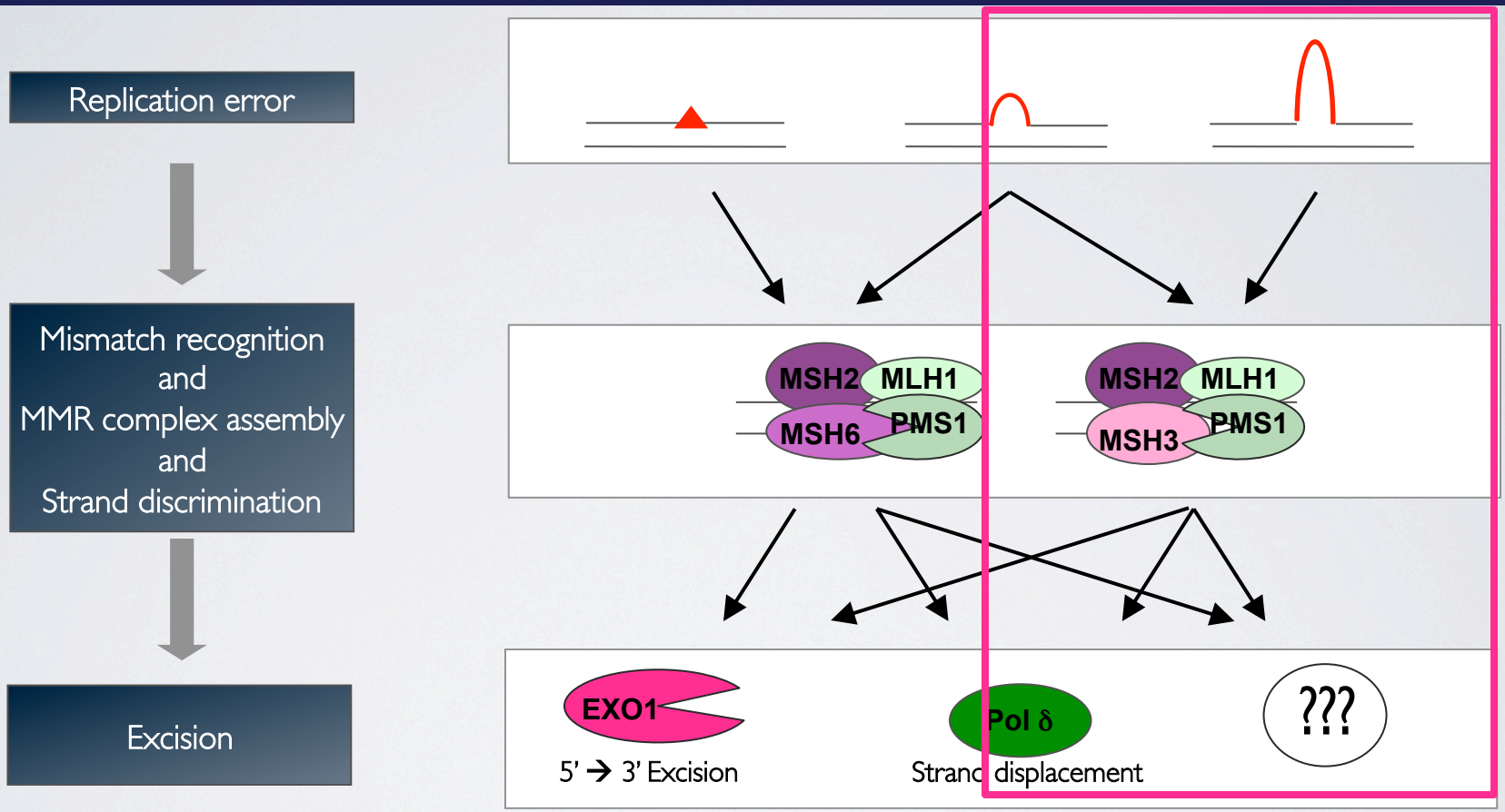

Hypothesis:

Exo1 is not significantly involved in repair of replication errors through the Msh2-Msh3 sub-pathway of MMR

Dissection of Exo1's functions in MMR sub-pathways

Replication error

Mismatch recognition
and
MMR complex assembly
and
Strand discrimination

Excision

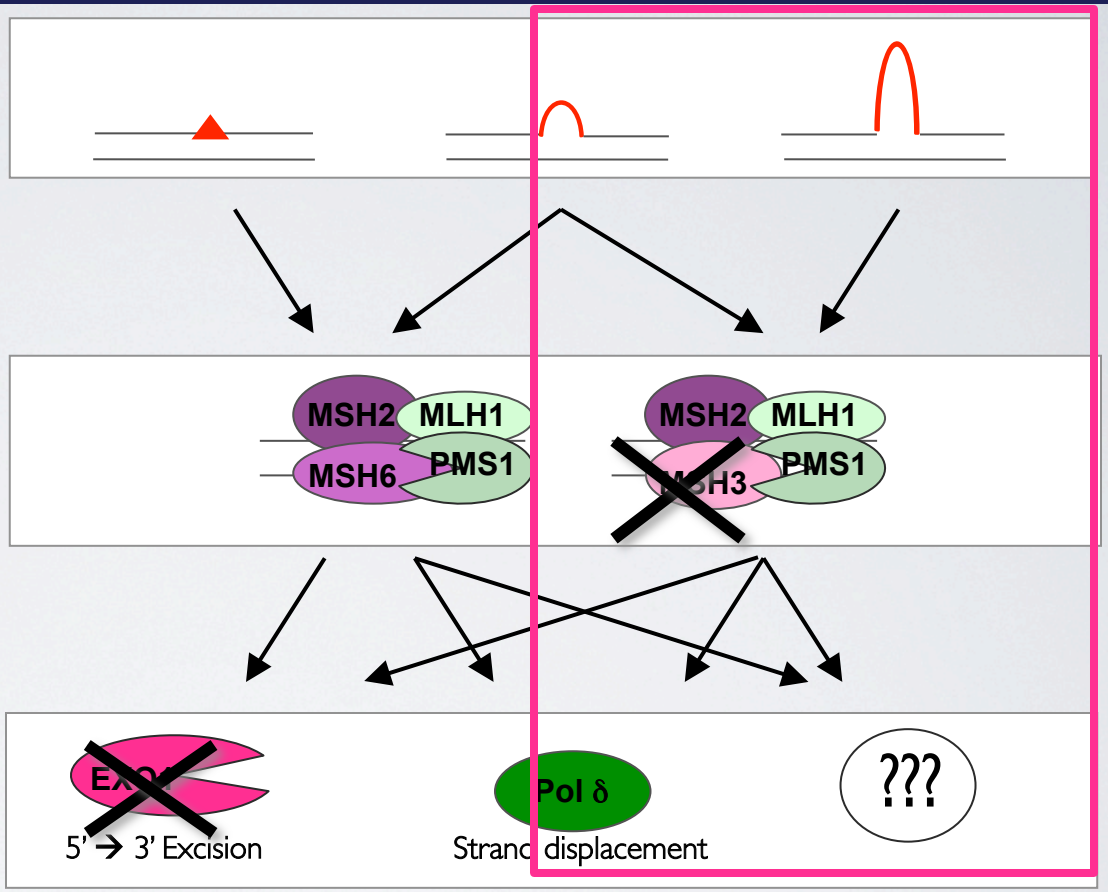

Mutation Specificity in *exo1Δ and msh3Δ* strains

MMR of –T in a run of Ts in *pol3-L612M*

Strain	Rate ($\times 10^{-7}$)
MSH2	0.006
msh2Δ	37
msh6Δ	0.54
msh3Δ	0.05
msh3Δ msh6Δ	19 (**synergy**)

Mutation Specificity in *exo1Δ and msh3Δ* strains

MMR of –T in a run of Ts in *pol3-L612M*

Strain	Rate ($\times 10^{-7}$)
MSH2	0.006
msh2 Δ	37
msh6 Δ	0.54
msh3 Δ	0.05
msh3 Δ msh6 Δ	19 (**synergy**)

Mutation Specificity in *exo1Δ and msh3Δ* strains

MMR of –T in a run of Ts in *pol3-L612M*

Strain	Rate ($\times 10^{-7}$)
MSH2	0.006
msh2Δ	37
msh6Δ	0.54
msh3Δ	0.05
msh3Δ msh6Δ	19 (**synergy**)
exo1Δ	0.10
exo1Δ msh3Δ	1.2 (**synergy**)

Exo1 preferentially participates in the Msh2•6-dependent MMR pathway

Summary

Exo1 in MMR

- Exo1 differentially repairs Pol **α** errors more efficiently than pol **δ** errors

- Exo1 dependent MMR plays a greater role in repairing lagging strand errors compared to leading strand errors

- Exo1 is involved in the Msh2-Msh6 sub-pathway of MMR

- In the absence of Exo1 most replication errors can still be corrected in an Msh2- dependent manner

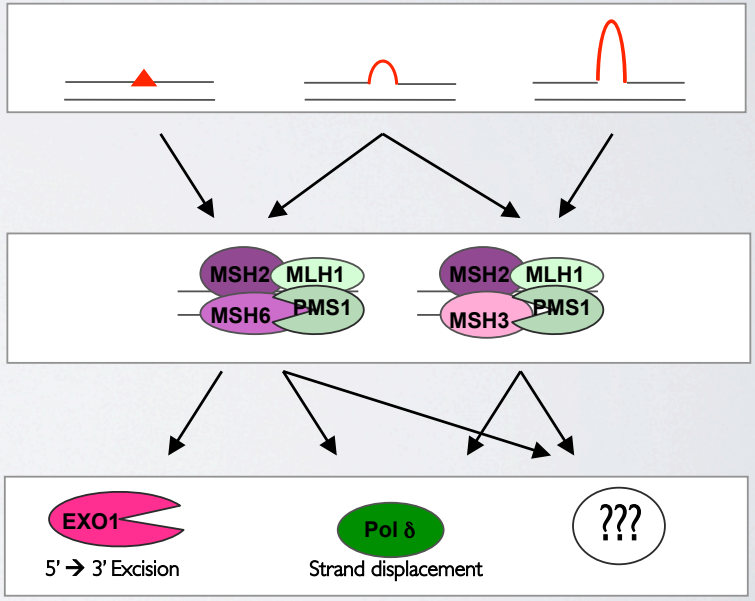

NIEHS
National Institute of Environmental Health Sciences

Acknowledgements

The DNA Replication Fidelity Group

Thomas Kunkel

Kasia Bebenek
Jessica Williams
Anders Clausen
Alan Clark
Mercedes Arana
Danielle Watt
Scott Lujan
Andres Larrea*

Laboratory of Molecular Genetics

Laboratory of Structural Biology

NIEHS

*former member

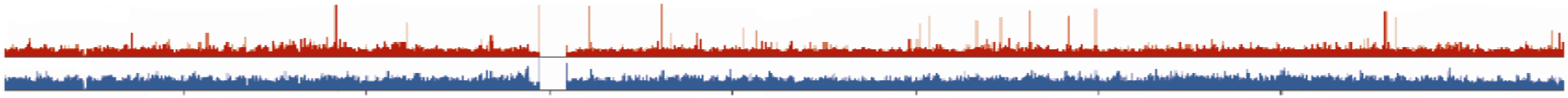

First High-Resolution Genome-Wide Map of p53 Binding Sites in Normal Human Cells

Krassi Botcheva,
Brookhaven National Laboratory, Upton, NY

VIDEOCONFERENCE
NIH DNA REPAIR INTEREST GROUP

Origin of Videoconference: BNL
TUSDAY JUNE 19 2012 12:30PM

First High-Resolution Genome-Wide Map of p53 Binding Sites in Normal Human Cells

Krassimira Botcheva

Assoc Geneticist
Brookhaven National Laboratory, Upton, NY

The rise of p53

Bert Vogelstein and Carol Prives

2009 Nature Reviews Cancer 9

↗ Inactivation of p53 is essential for the formation of nearly all cancers.

↗ The volume of work on p53 has shown it to be at the centre of a cellular network of feedback and feedforward loops, forming a paradigm for system biology.

↗ Understanding of this network, and determining how it can be exploited for therapeutic benefit, will keep scientists busy for years to come.

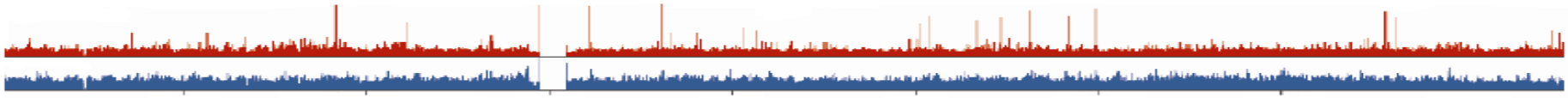

↗ Upon DNA damage p53 binds to the genome and regulates transcription of extensive network of genes, promoting cell cycle arrest, DNA repair, senescence or apoptosis.

↗ Unresolved remains the question how p53 discriminates between the thousands of potential p53 binding sites predicted in the human genome.

↗ Individually analyzed functional binding sites are close to the target genes/TSS.

↗ Three major genome-wide studies were published in human cancer-derived cells.

Chip-PET, HCT116, Wei et al, Cell 2006
ChIP-chip, U2OS, Smeenk et al. NAR 2008
ChIP-seq, U2OS, Smeenk et al. PLOS 2011

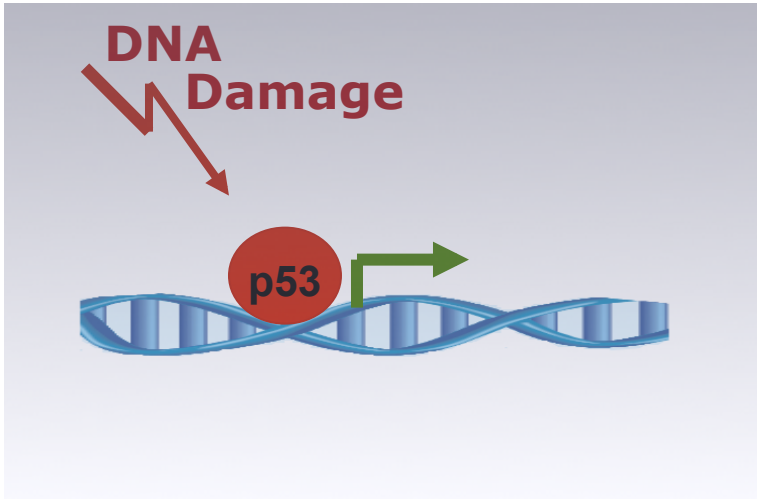

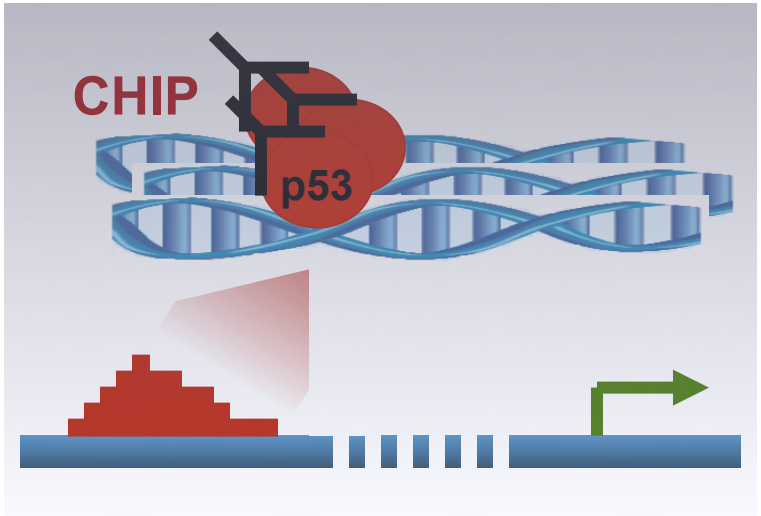

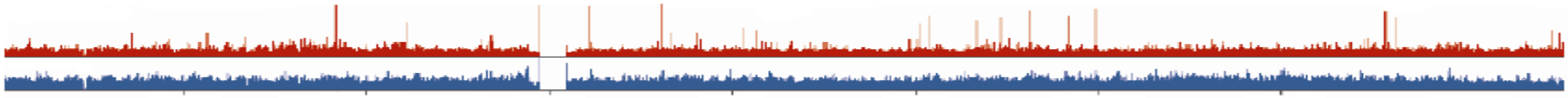

Where in the genome binds p53 in normal not transformed human cells?

Are these locations similar or different from those reported previously in cancer-derived cell lines?

What is the genomic landscape of the p53 binding sites?

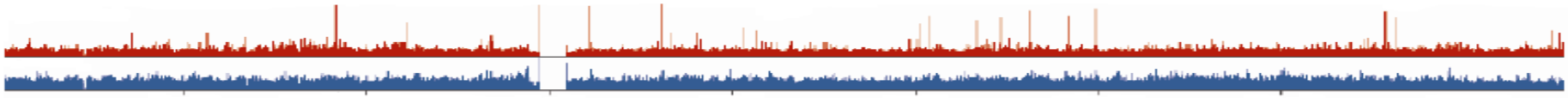

Defining high-confidence p53 binding sites in normal human fibroblasts IMR90

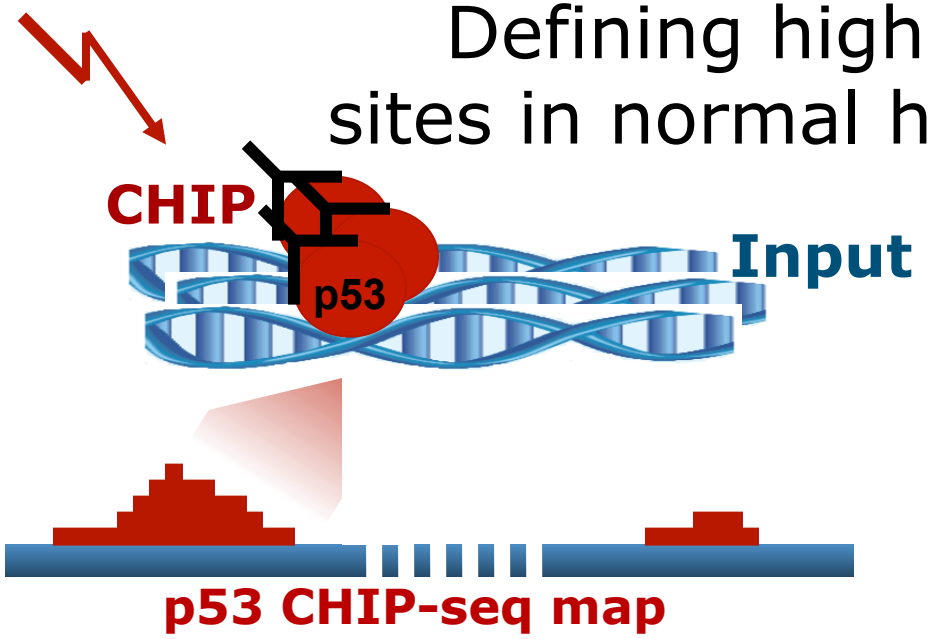

NGS Illumina

Distinct unique reads

ChIP-seq	Input-seq
~4 million	~8 million

Total number of peaks

~6,800	~2,500

Enriched above Input

~1,700 ChIP-seq peaks

High-confidence

743 ChIP-seq peaks

qPCR validation

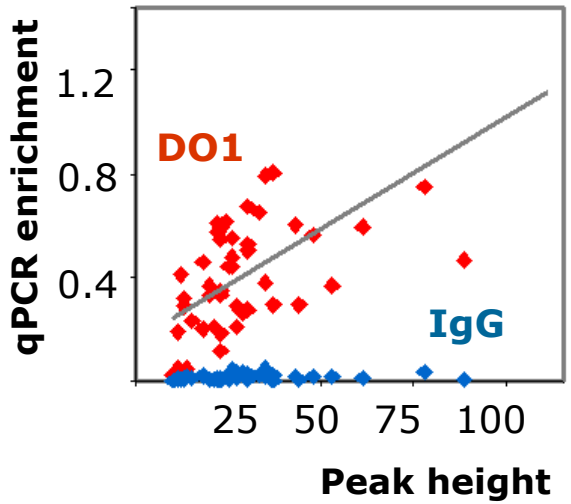

p53 ChIP-seq and Input-seq map at chr6 and the canonical p53 target CDKN1A

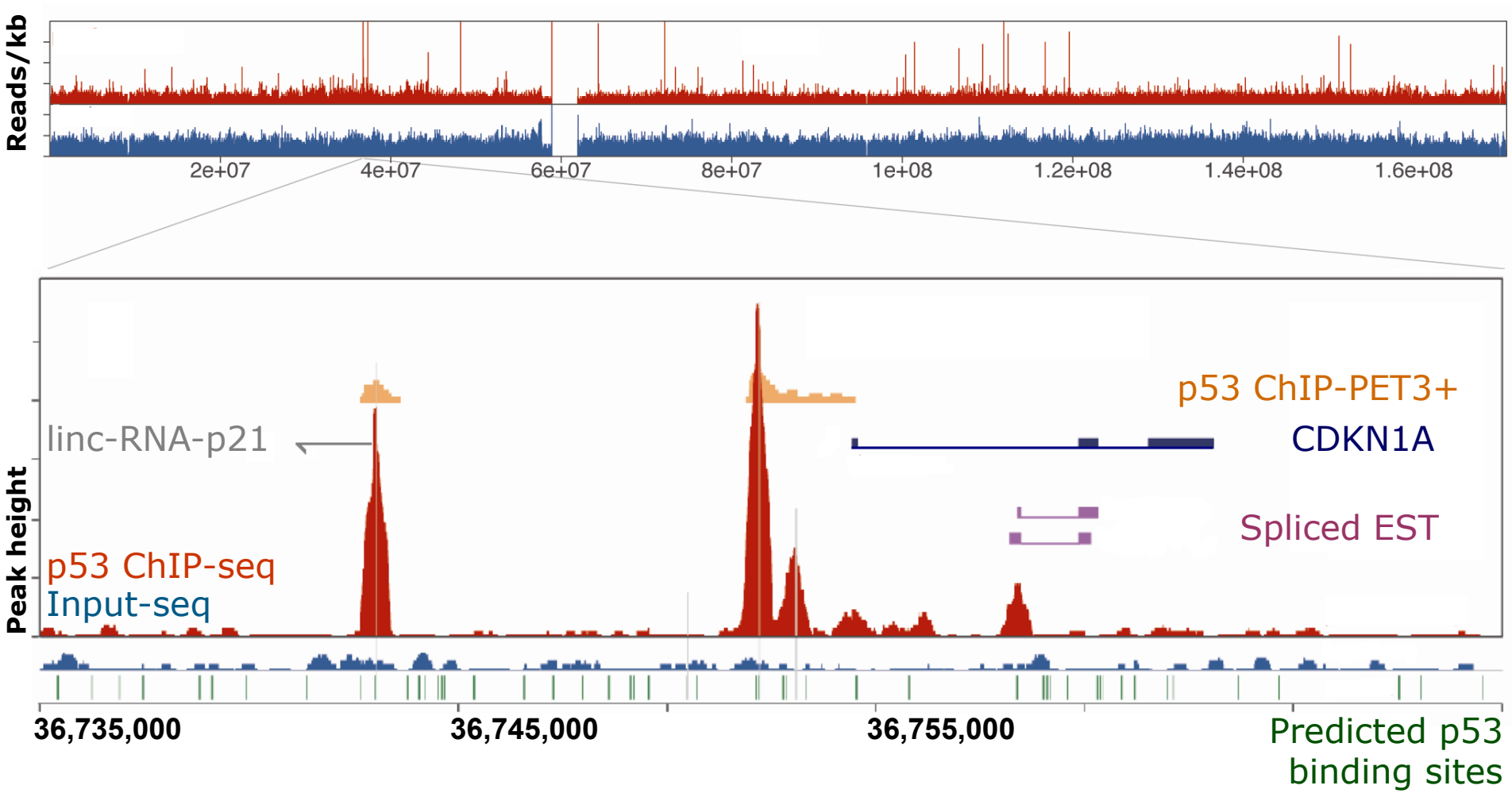

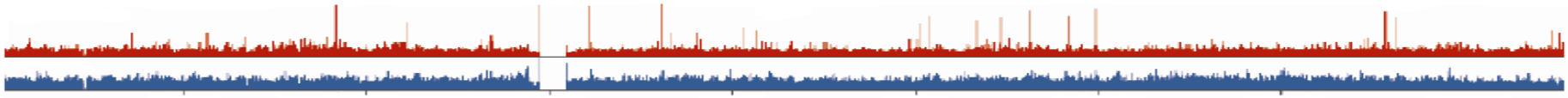

Out of 168 known functional (reference) p53 binding sites, 62 were successfully identified in IMR90

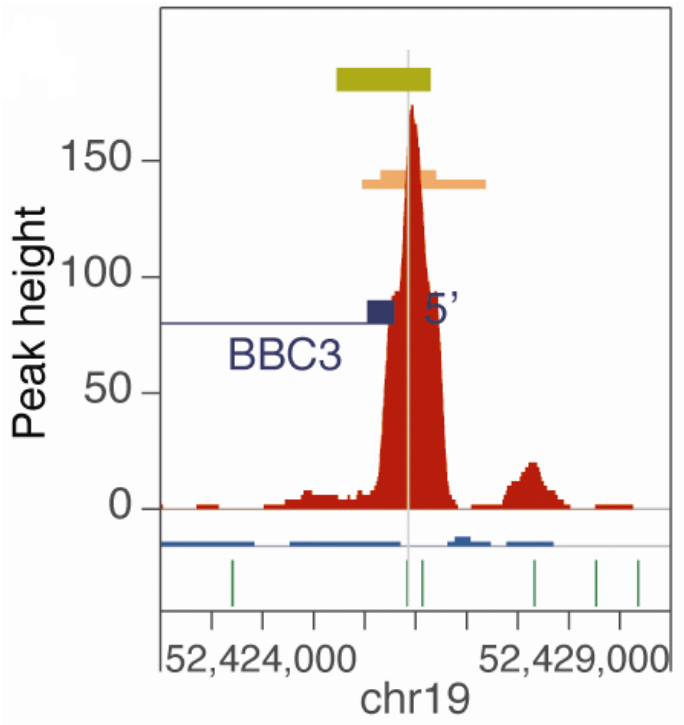

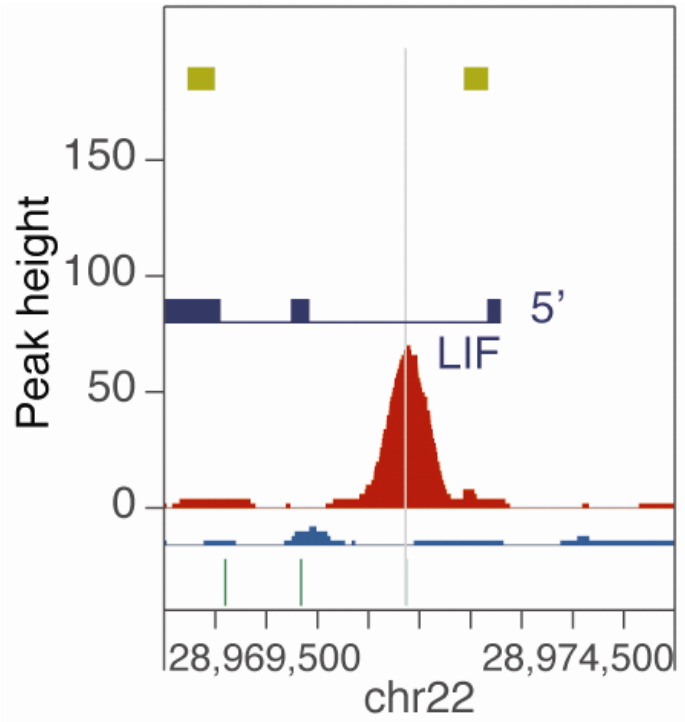

For 79% of the identified reference sites, the distance between the peak maximum and the reference site center was less than 50 nt, and for 52% - less than 20 nt.

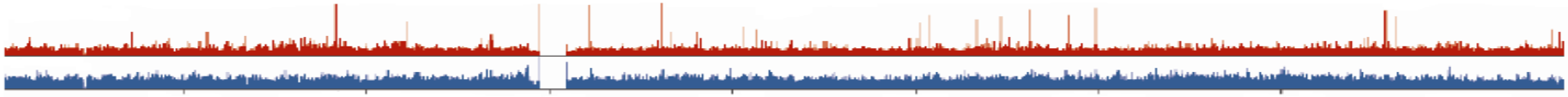

p53 ChIP-seq peaks are strongly enriched for predicted p53 binding sites and for TSS

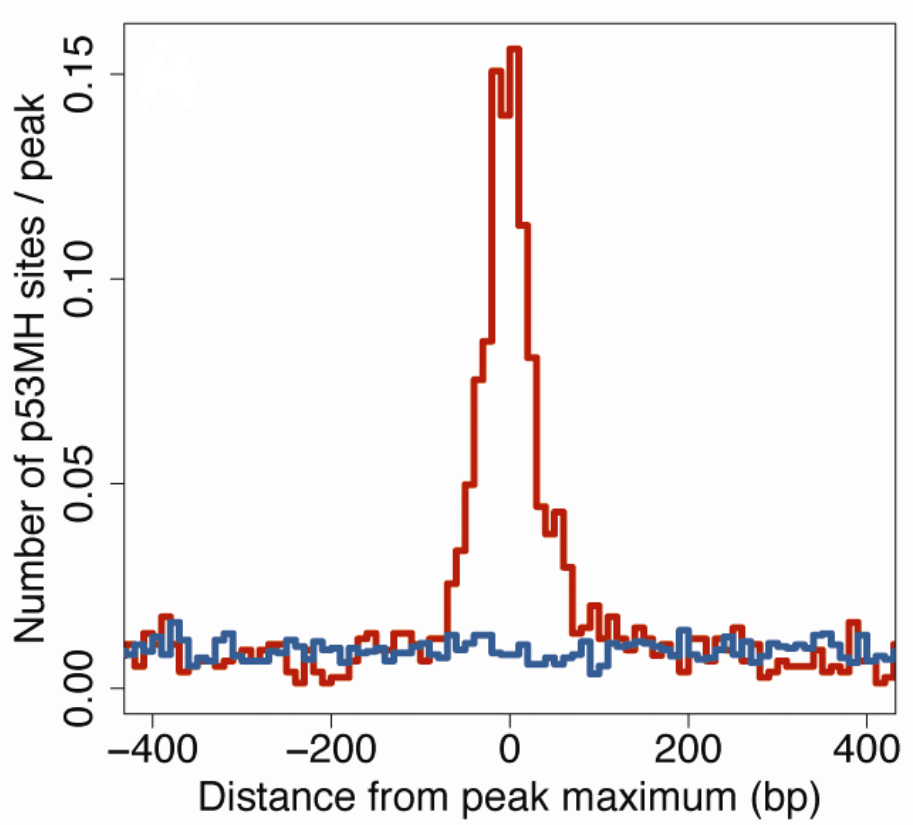

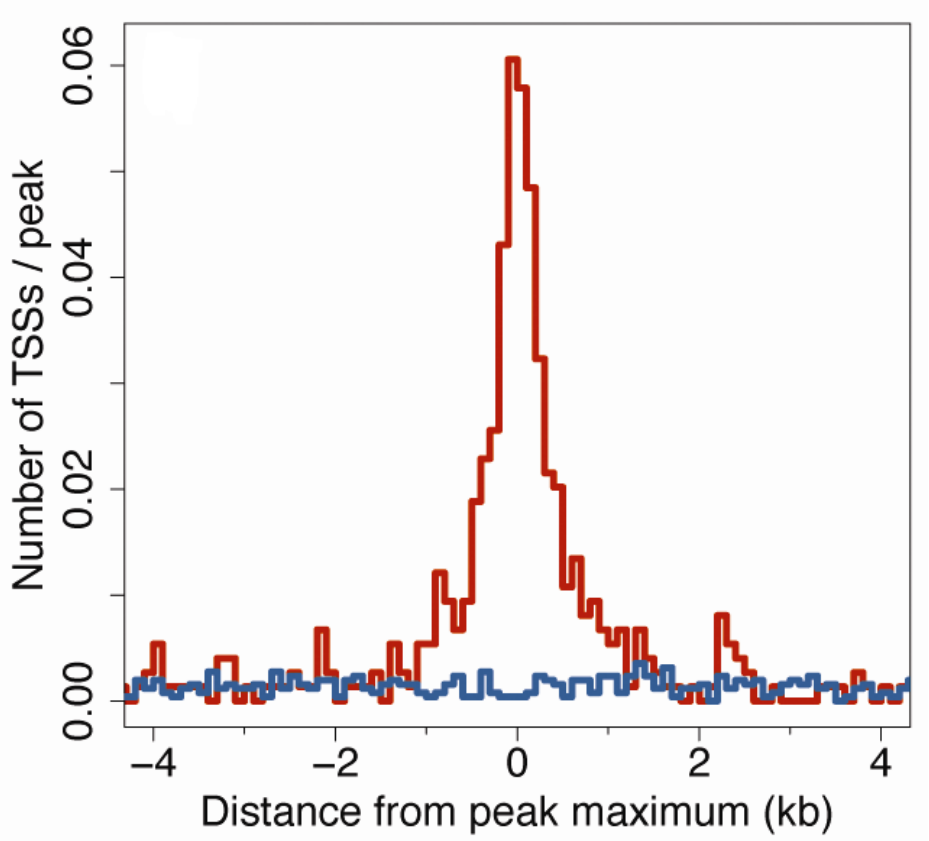

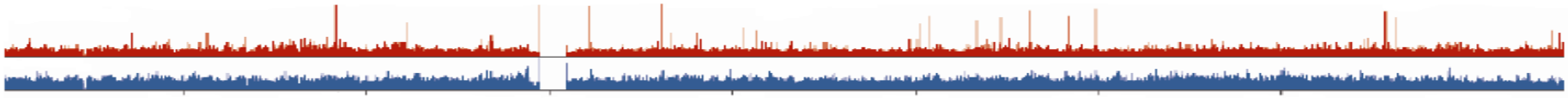

Only in the normal IMR90 cells p53 ChIP-seq peaks are strongly enriched at TSS and CpG islands (CGIs)

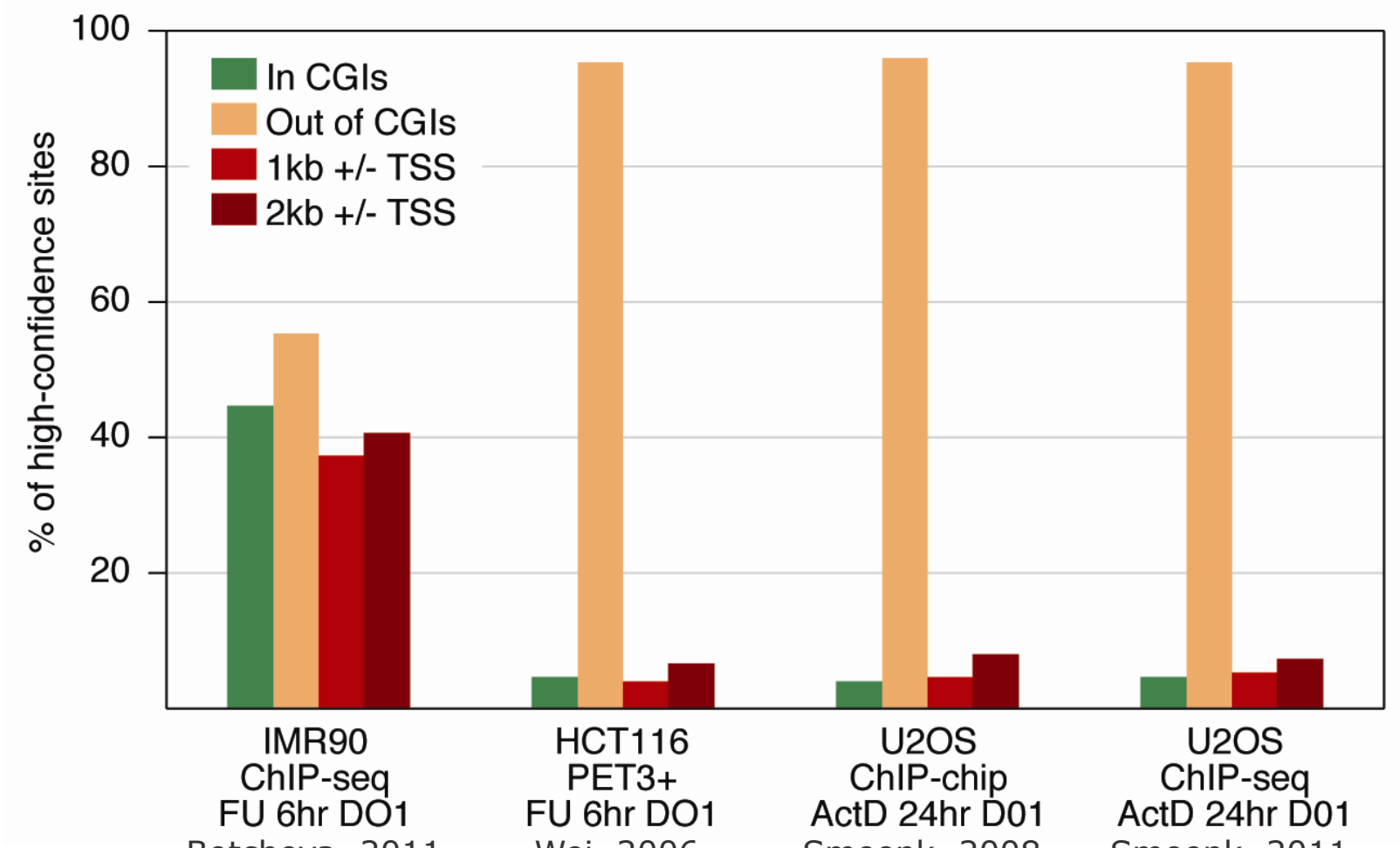

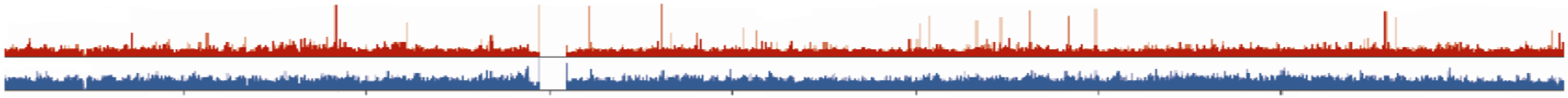

In IMR90 cells p53 ChIP-seq peaks are enriched for CpGs and at hypomethylated DNA

p53 ChIP-seq peaks are enriched for CpG dinucleotides

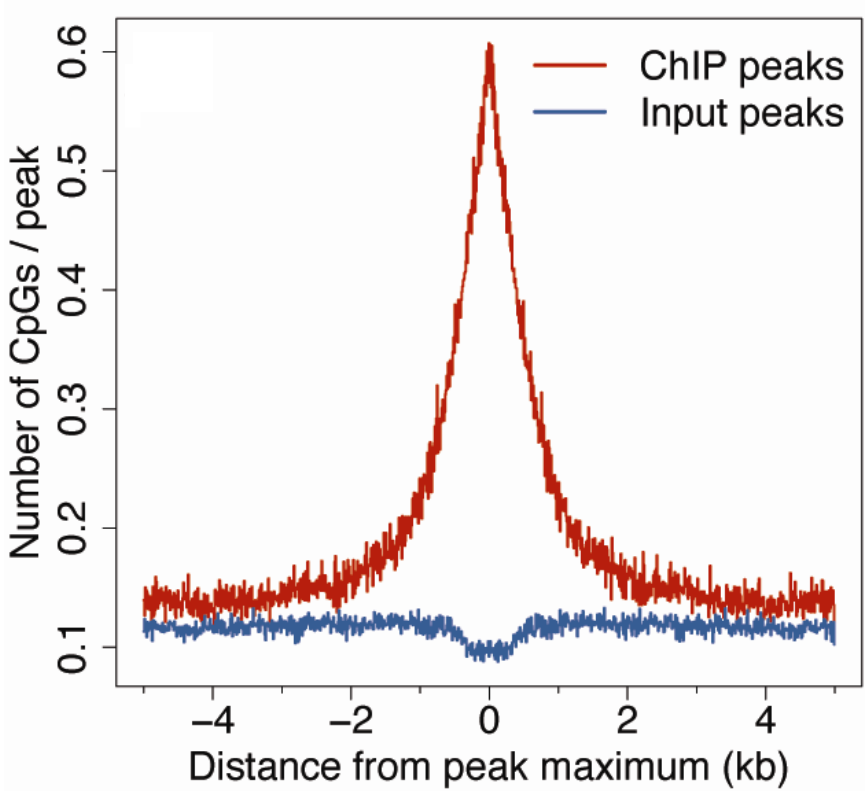

p53 ChIP-seq peaks are hypomethylated

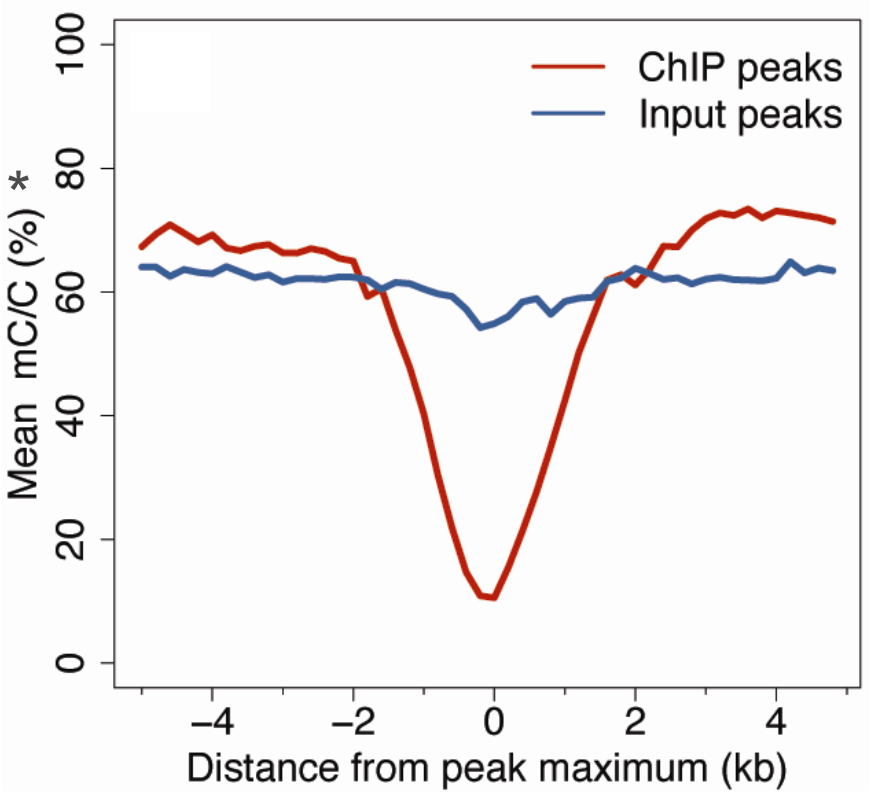

* IMR90 methylation data from Lister et al. Nature, 2009.

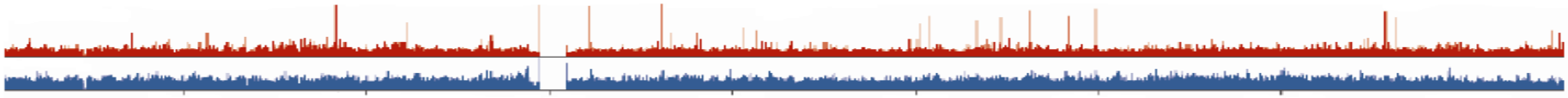

p53 ChIP-seq peaks in CGIs and out of CGIs have different hypomethylation profile

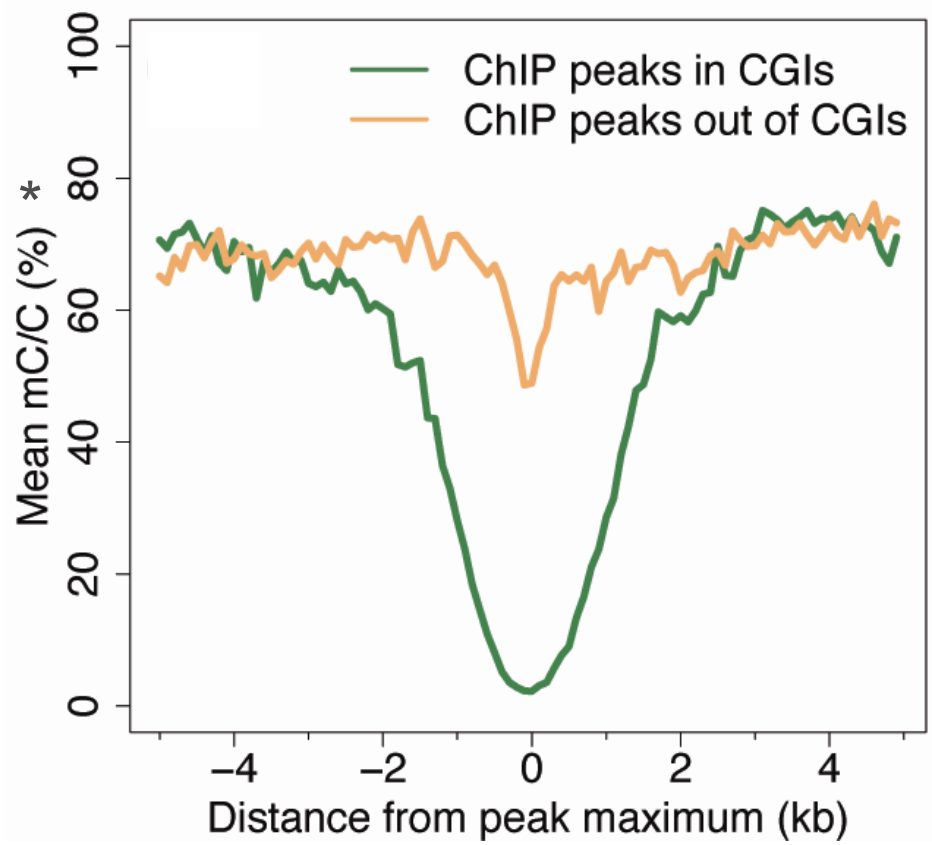

* IMR90 methylation data from Lister et al. Nature, 2009.

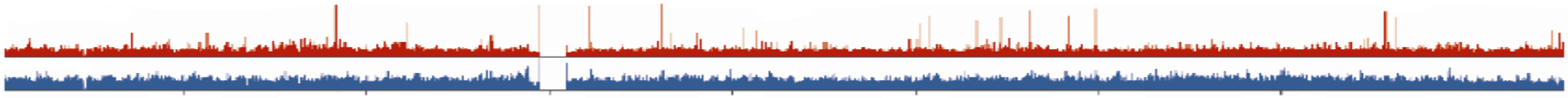

In IMR90 cells p53 ChIP-seq peaks are enriched at proximal CpG islands

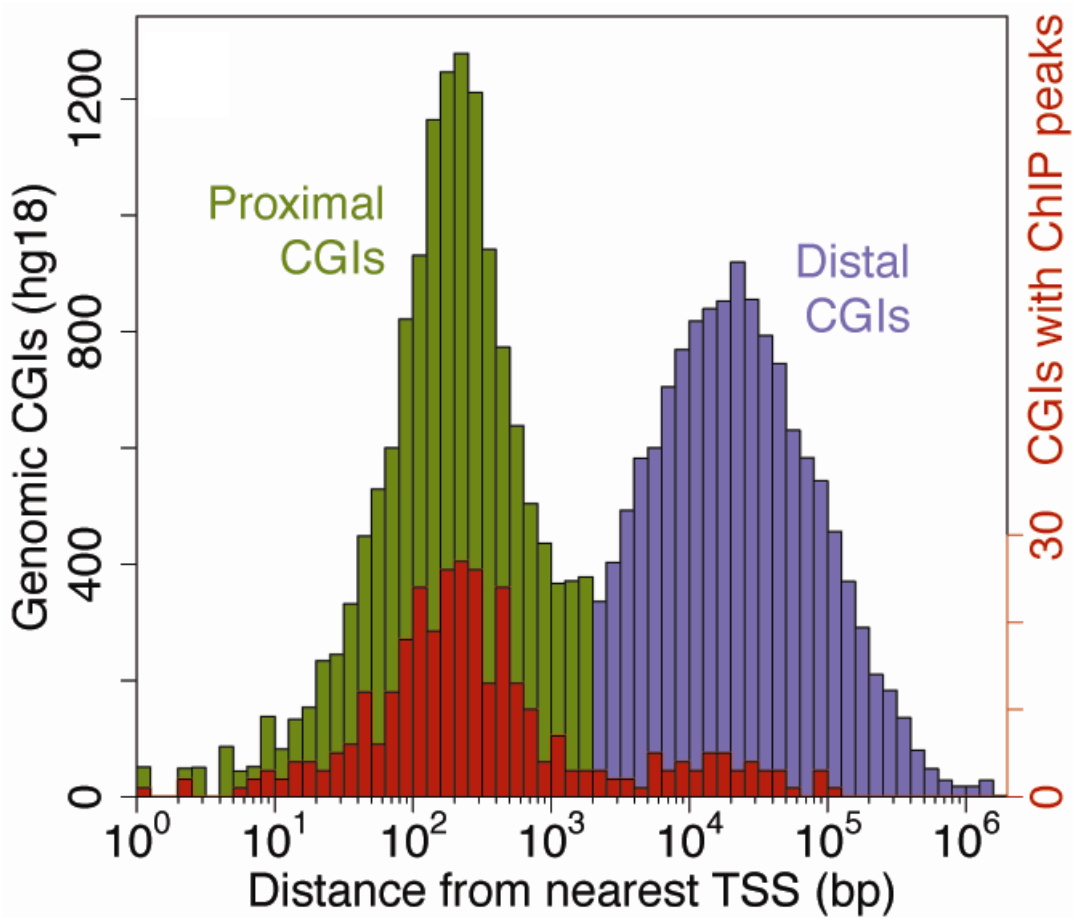

Distribution of all human CGIs with respect to TSS. Plotted in red are CGIs at which high-confidence p53 ChIP-seq peaks are found.

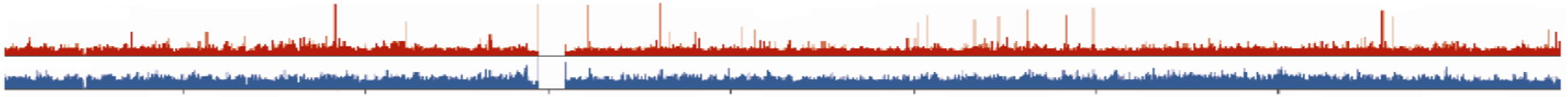

In IMR90 cells p53 ChIP-seq peaks are enriched at hypomethylated DNA

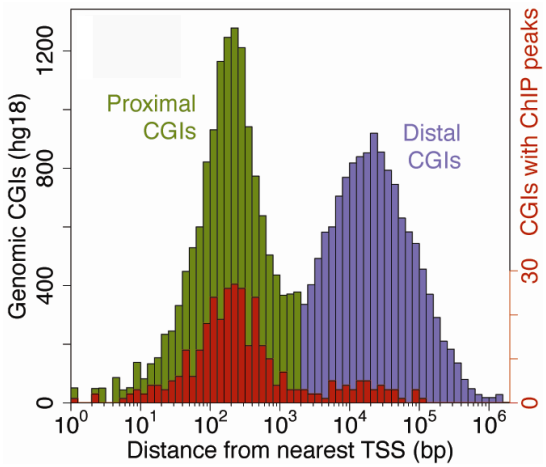

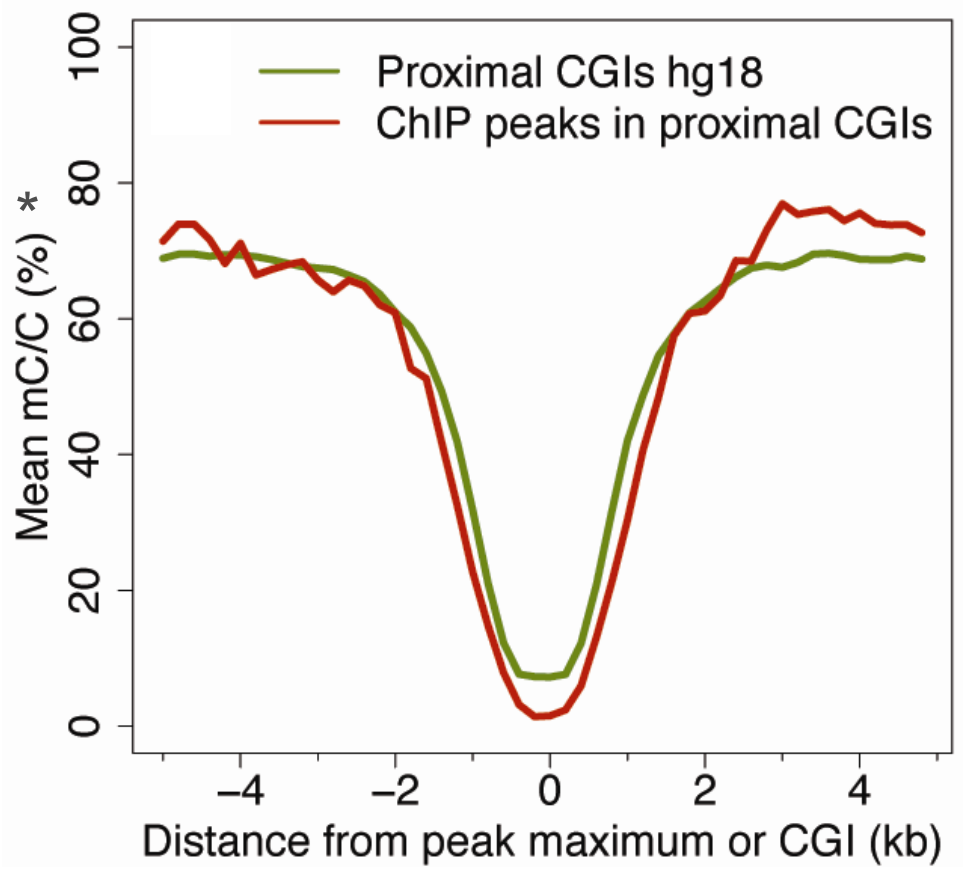

* IMR90 methylation data from Lister et al. Nature, 2009.

The hypomethylation level of ChIP-seq peaks in proximal CGIs matches that of all human proximal CGIs.

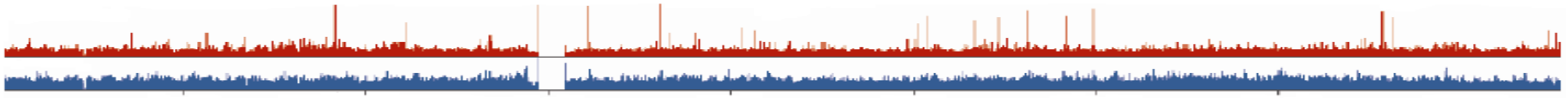

In IMR90 cells p53 ChIP-seq peaks are enriched at hypomethylated DNA

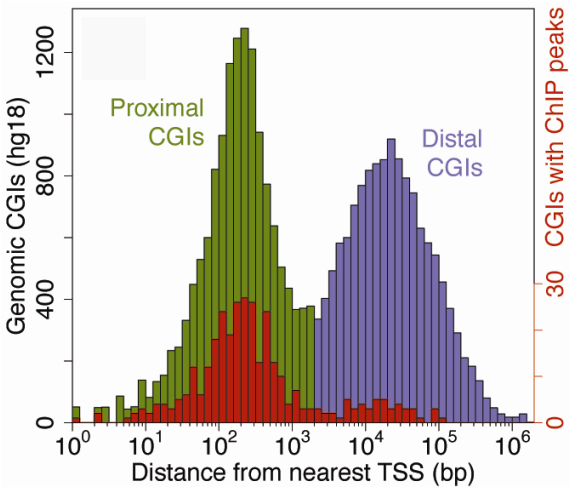

* IMR90 methylation data from Lister et al. Nature, 2009.

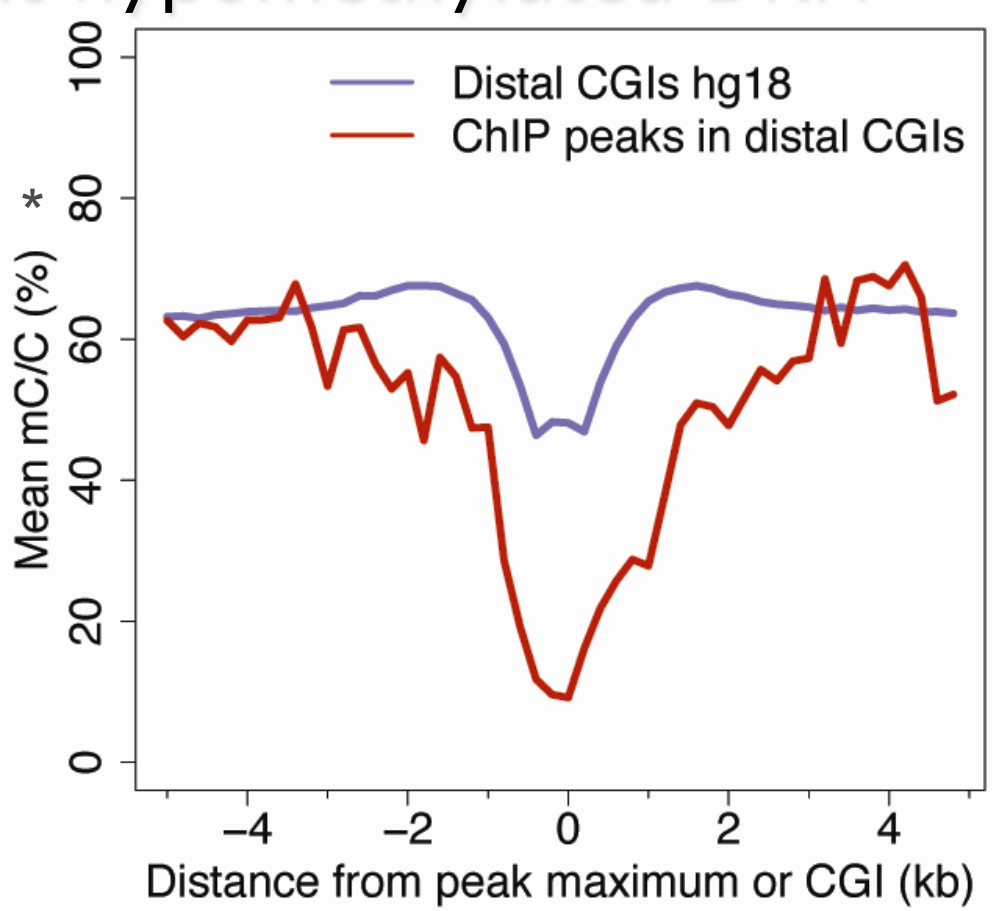

p53 ChIP-seq peaks in distal CGIs are more hypomethylated than the human distal CGIs.

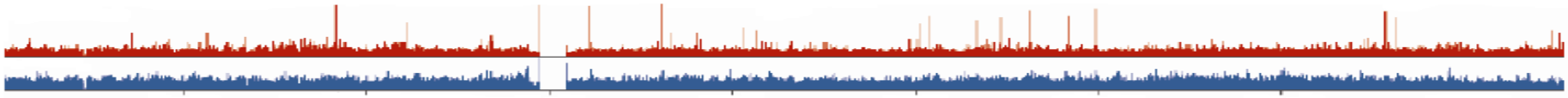

Motif analysis of the high-confidence ChIP-seq peaks identified in IMR90 cells

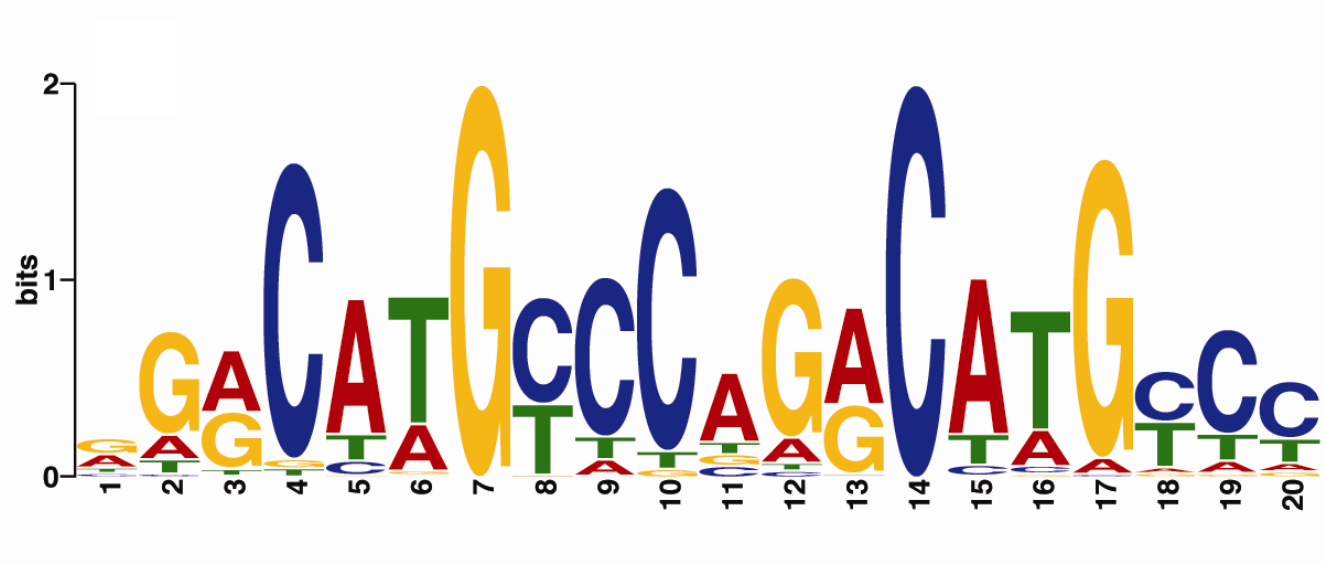

Sequence logo depicting the p53CSI motif (ChIP-seq identified in IMR90), E-value 1.2e-1059.

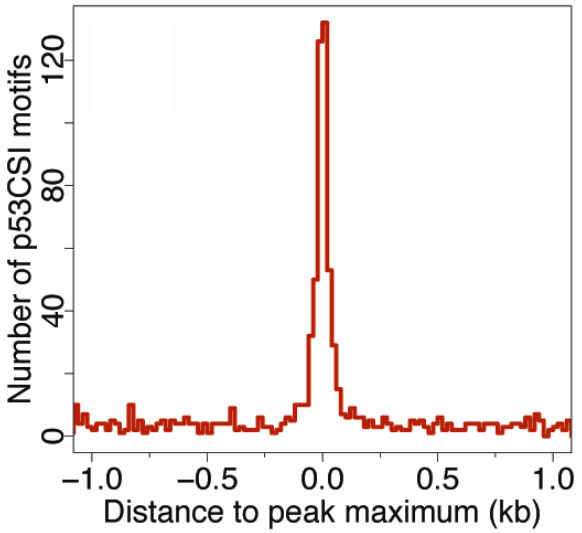

p53 motif enrichment at the ChIP-seq peaks

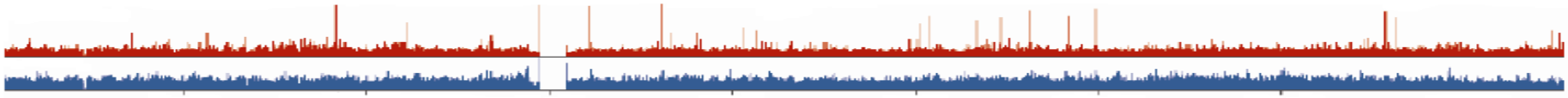

Summary

p53 binding sites in the cancer cells HCT116 and U2OS

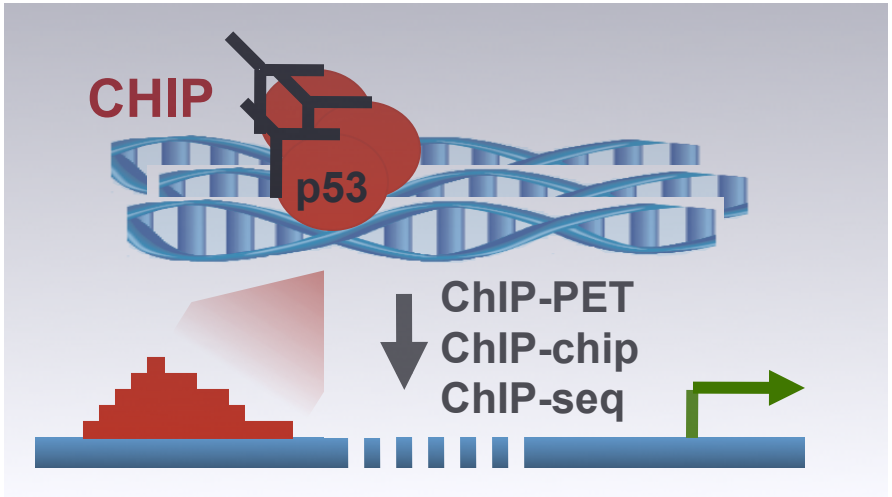

- Less than 5% within 2kb of TSS
- Depleted from CGIs
- Enriched at repeats
- Methylation status ?

p53 binding sites in the normal cells IMR90

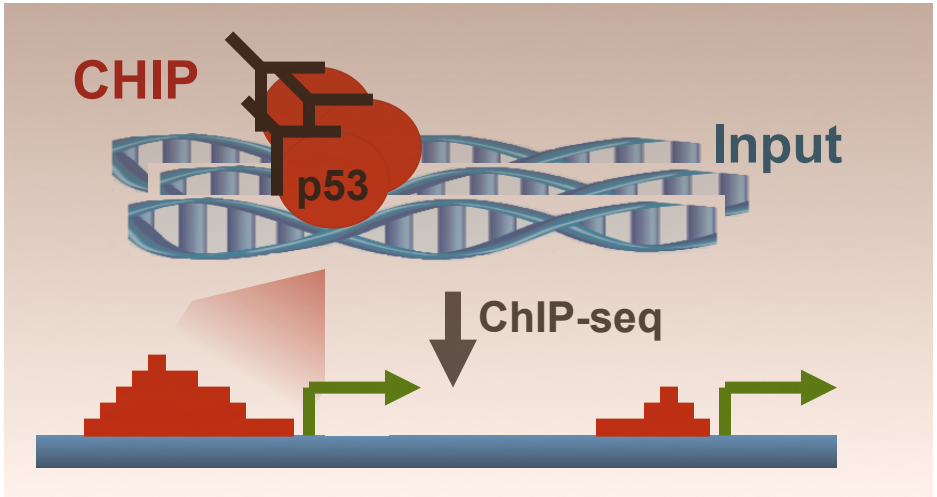

- More than 40% within 2kb of TSS
- Strongly enriched at CGIs
- Less enriched at repeats
- Hypomethylated

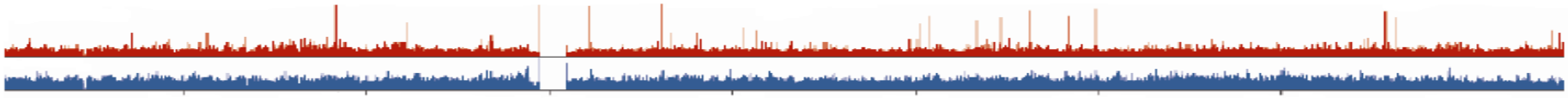

Summary

- We provide high-resolution genome-wide map of p53 binding sites in normal (not transformed) human cells.

- These sites have distinct genomic distribution compared to those previously reported in cancer-derived human cells.

- That distribution does not reflect p53 affinity to specific sequences.

- A small fraction of binding sites is present in all four p53 datasets analyzed; only in the normal cells p53 is highly enriched within 2kb +/- TSS, distribution characteristic for the individually analyzed functional p53 binding sites.

- In the normal human cells p53 is highly enriched at CpG islands and hypomethylated DNA.

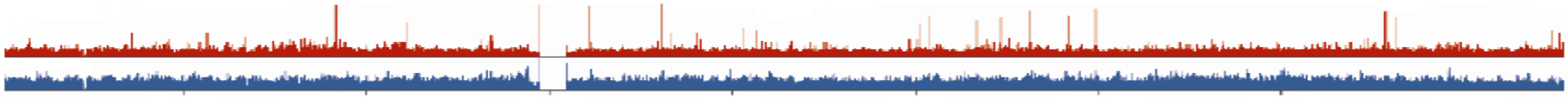

Open Questions

- How important for the p53 genome-wide binding is the epigenetic landscape of the human genome?

- How global hypomethylation and local CpG islands hypermethylation accompanying cancer development affect p53 genome-wide binding and target selectivity?

- How Low Dose Radiation and the epigenetic changes caused by it affect p53 binding and DNA damage response in the human cells?

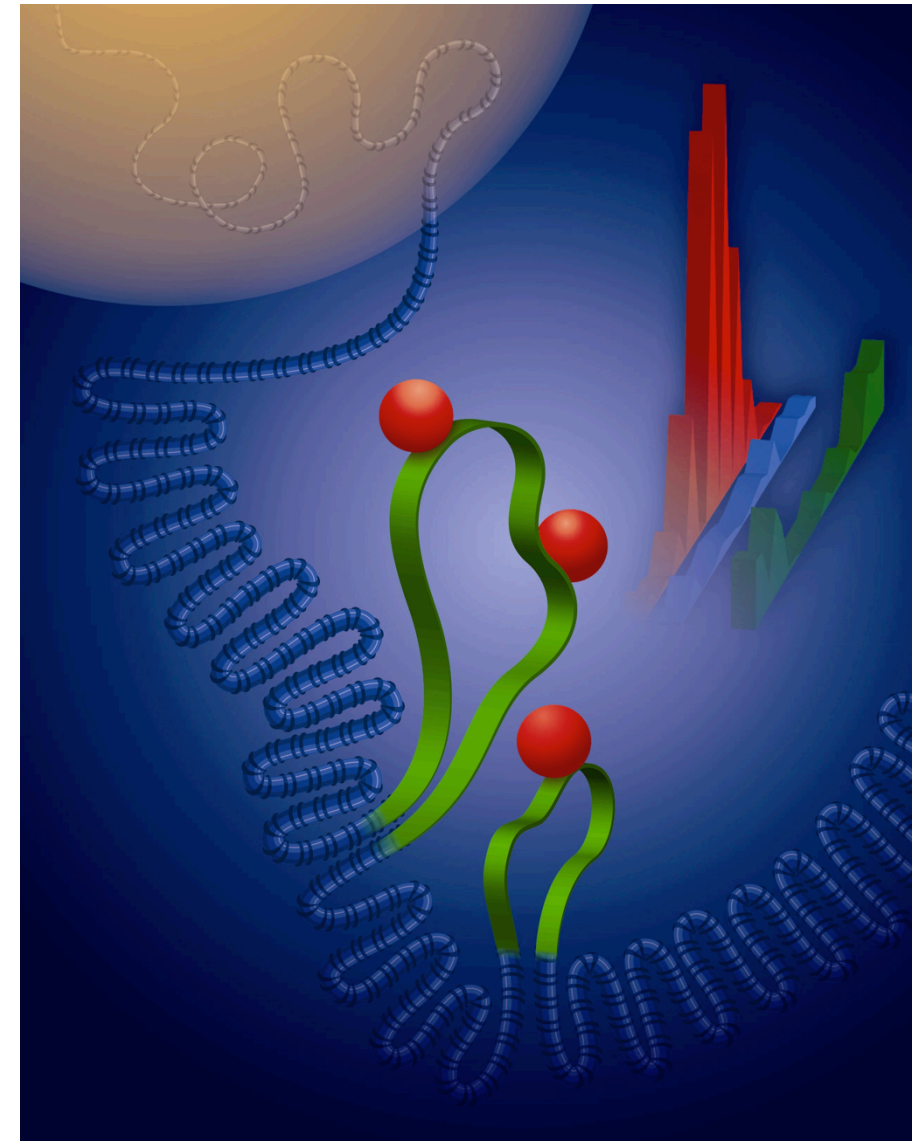

Acknowledgements

Sean McCorkle, BNL
Carl Anderson, BNL

John Dunn, BNL
Mike Blewitt, BNL

Dmitri Kotov, SULI student (BNL)

Dick McCombie, CSHL
Elena Ghiban, CSHL

David Turner, Sanger UK
Joel Rozowsky, Yale
Michael Regulski, CSHL

Paul Wilson, BNL

Tiffany Bowman (BNL, Graphic Design)

This work was supported by the Low Dose Radiation Program (DOE) and LDRD (BNL).

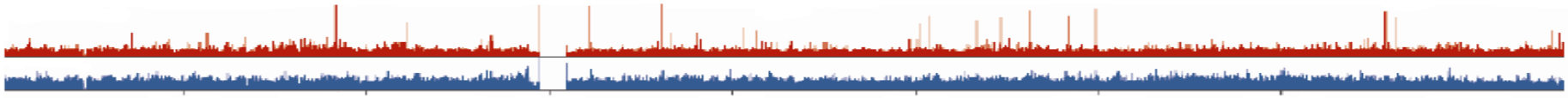

NEXT ?

Genome-wide studies on different types of cells (normal and cancer) combined with DNA methylation and histone modification maps, can help place p53 binding in the context of chromatin in vivo, to address the epigenetic impact on the p53 dependent transcription regulation and to provide a global view of the p53 network changes during cancer progression.

Botcheva et al. Cell Cycle 2011

Role of the Circadian Clock in UV-Induced Skin Carcinogenesis

Shobhan Gaddameedhi

Aziz Sancar Lab

Circadian Rhythm & Circadian Clock

***circa*, "around," *dies,* "a day"**

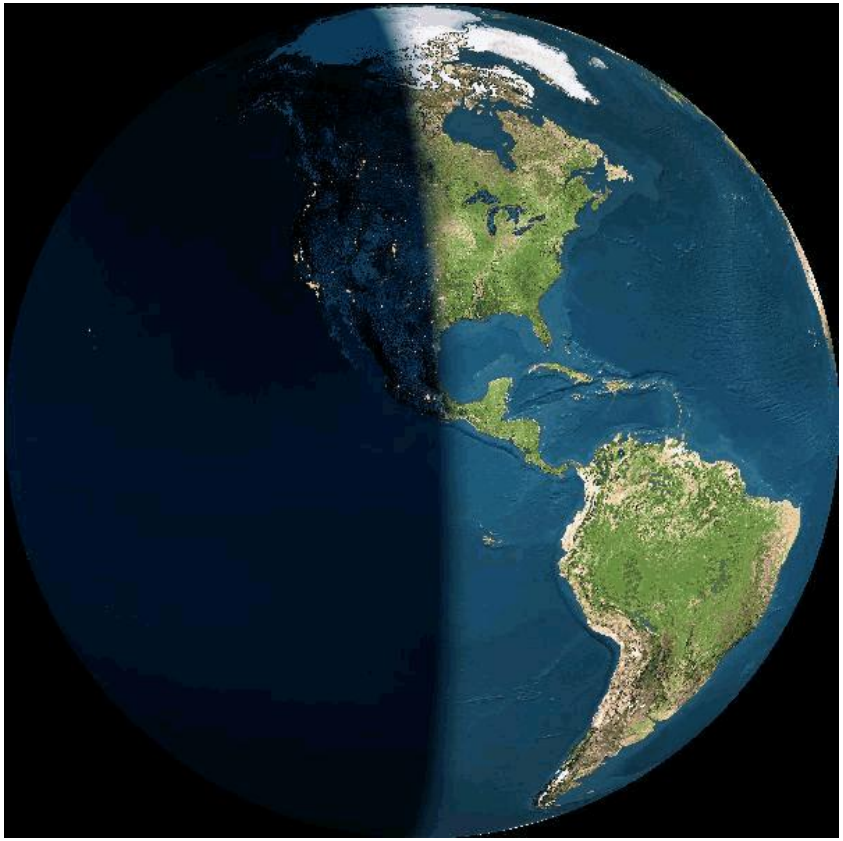

www.learner.org/jnorth/images

- Circadian Rhythm
- Circadian Clock
- Synchronized with the solar clock by light

Circadian clock disruption

- Sleep Disorder
- Jet Lag

Clock related diseases

- Cancer
- Heart attack
- Type 2 diabetes

Loss of Rhythmic Behavior in Clock-deficient Mice

Actogram: Wheel running activity

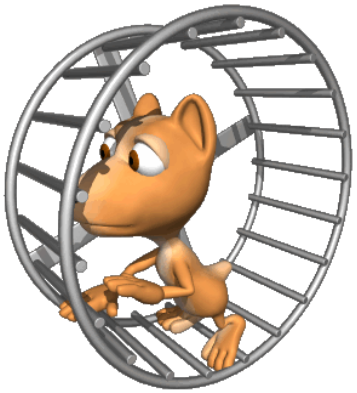

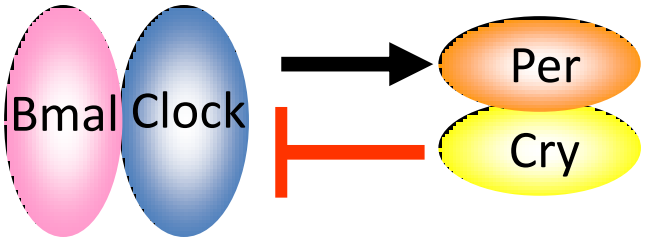

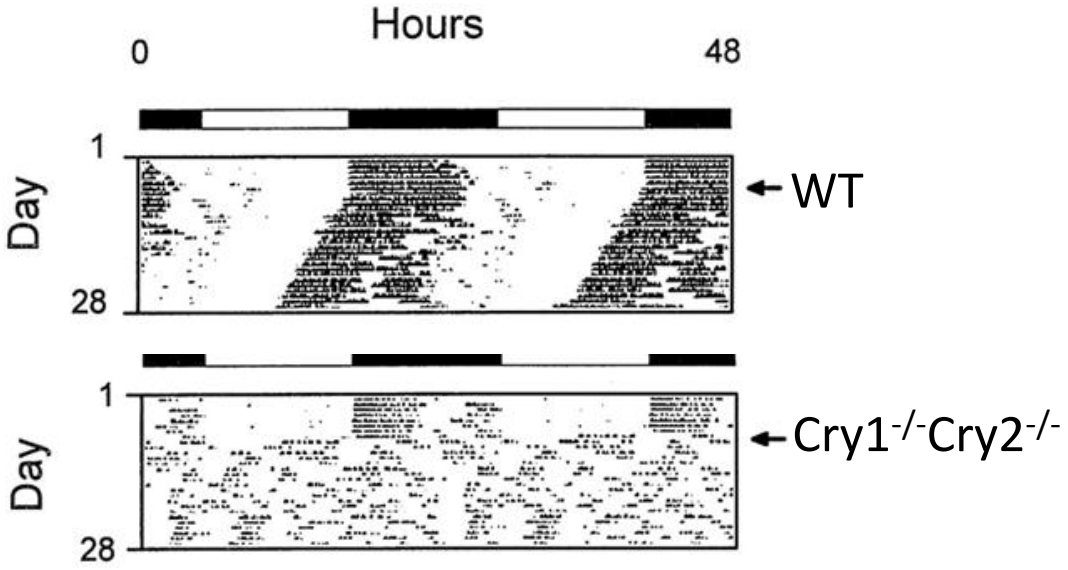

Vitaterna *et al.* PNAS **(1999)** 96, 12114-12119

Role of the Excision Repair in preventing UV-induced Skin Carcinogenesis

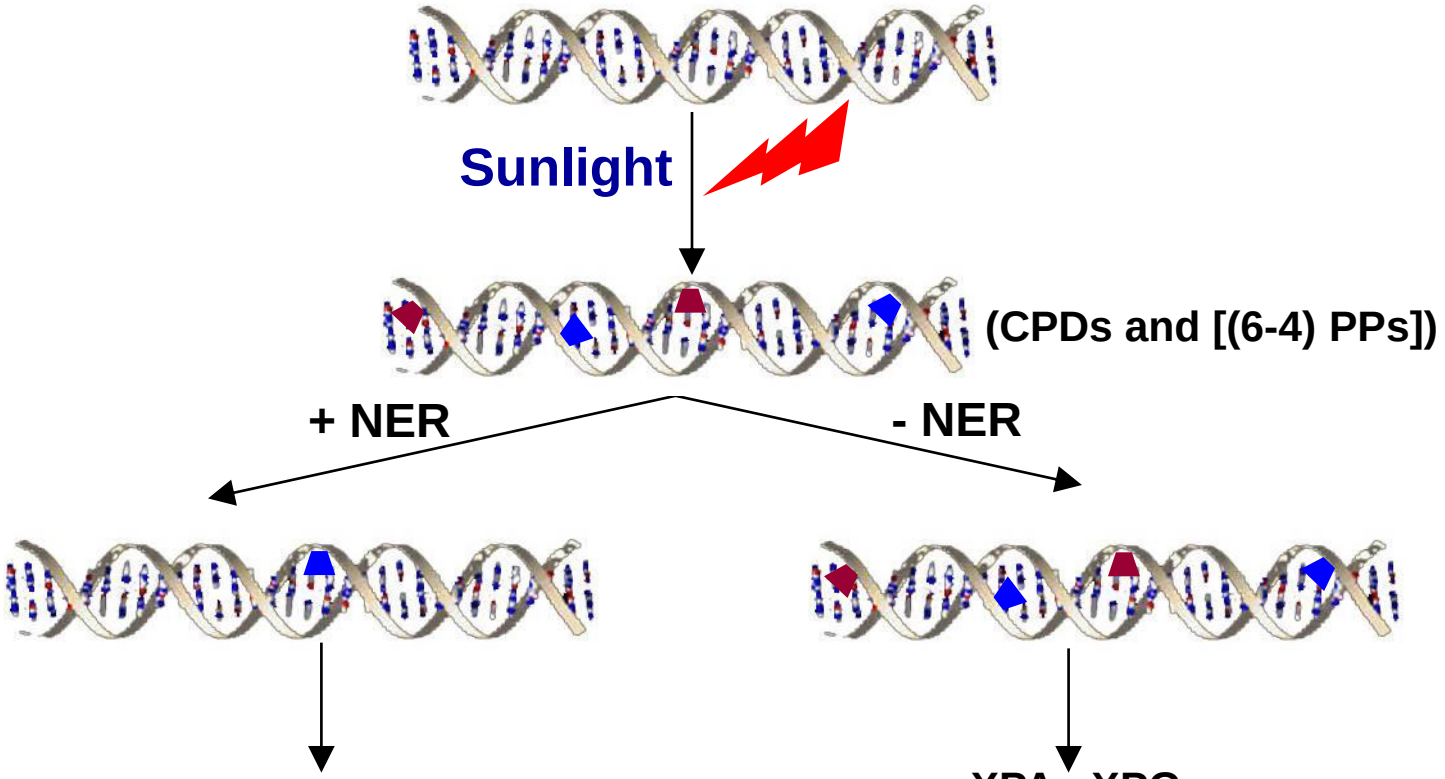

Wild Type
Proficient NER
Proficient lesion bypass
Basal mutagenesis

XPA - XPG
Defective NER
Proficient Lesion Bypass
(increased lesion load)
Increased mutagenesis
Skin cancer predisposition

Circadian Oscillation of NER Activity and XPA Levels in Mouse Liver and Brain

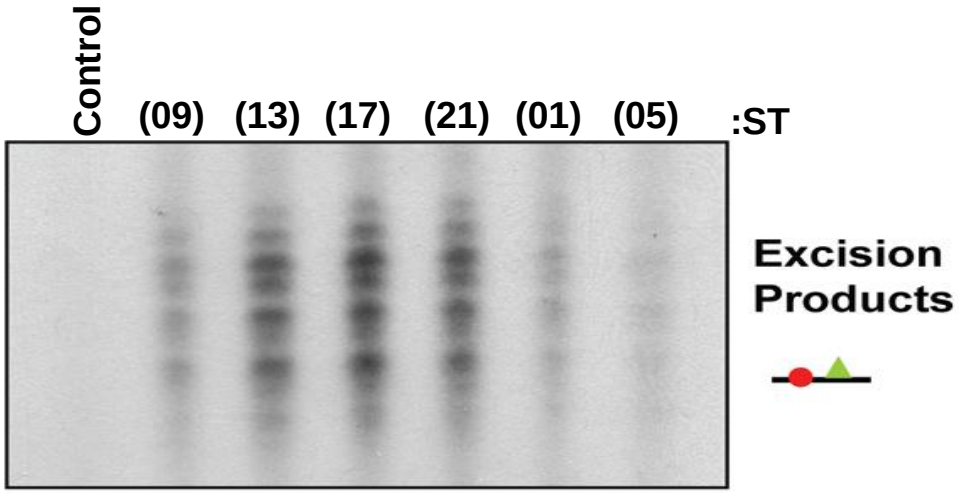

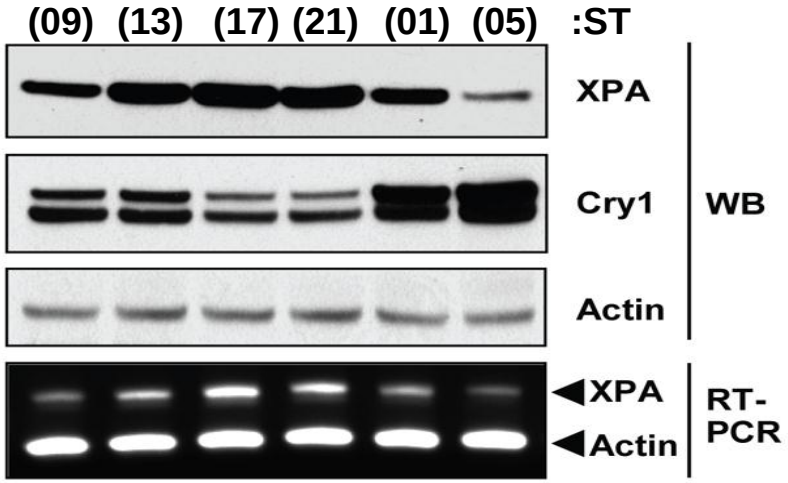

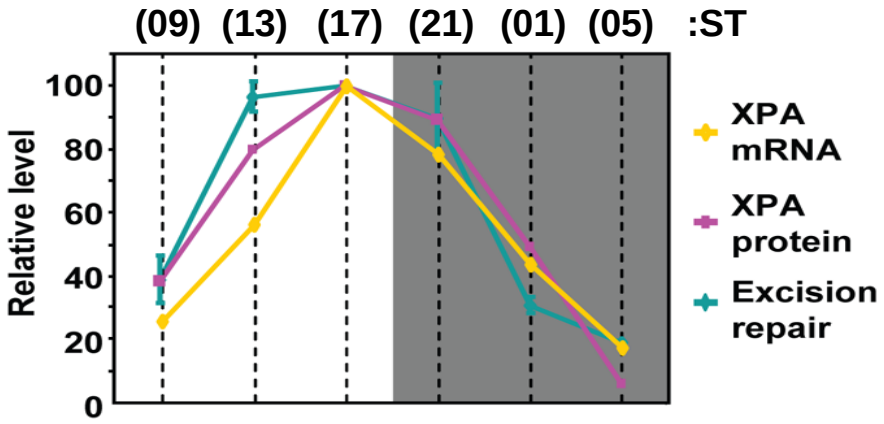

Kang T *et al.* **(2009)** PNAS 106, 2864-2867 and PNAS **(2010)** 107, 4890-4895.

Potential importance of Rhythmic Expression of NER Activity in Skin Cancer Incidence?

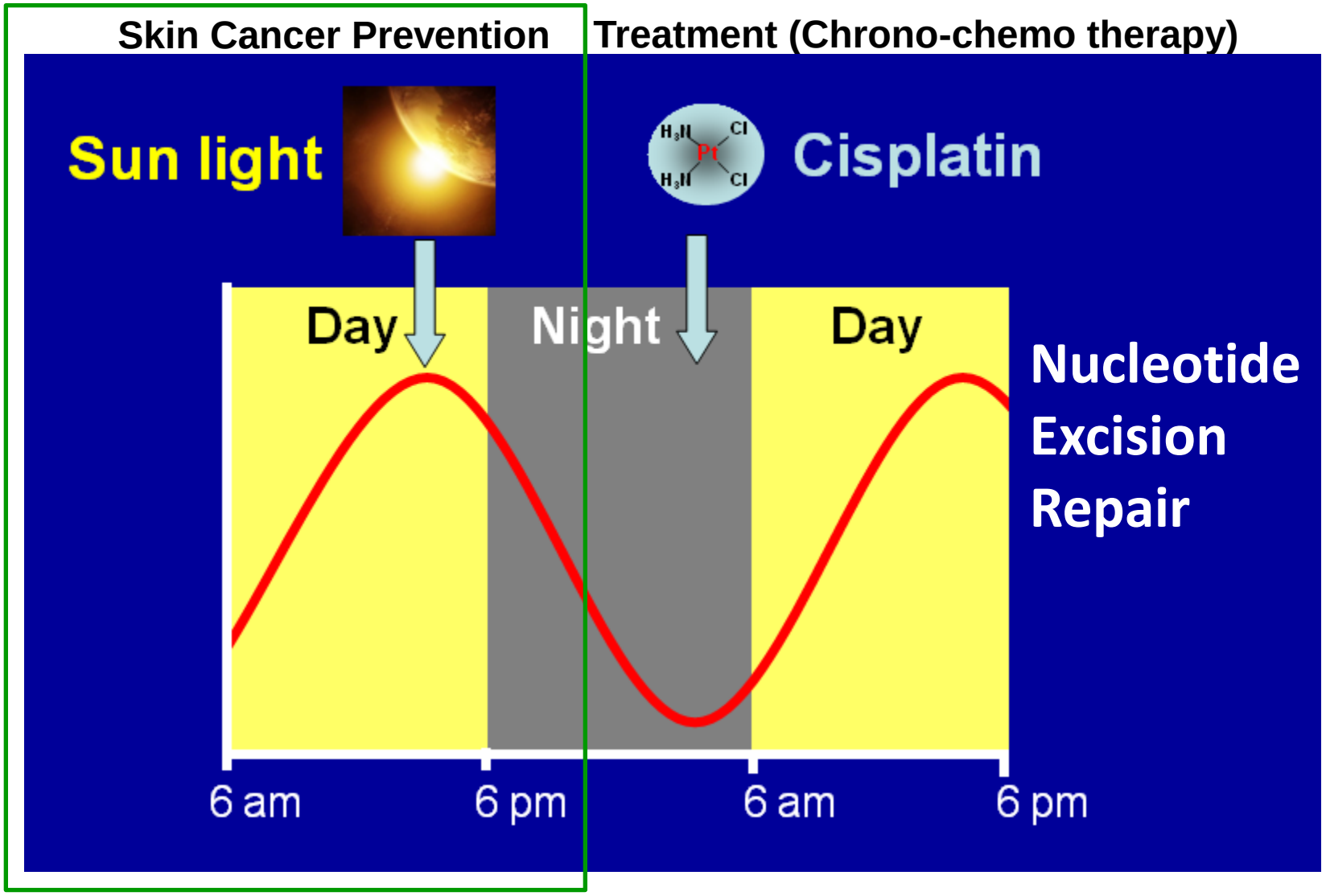

Circadian Oscillation of XPA in Mouse Skin

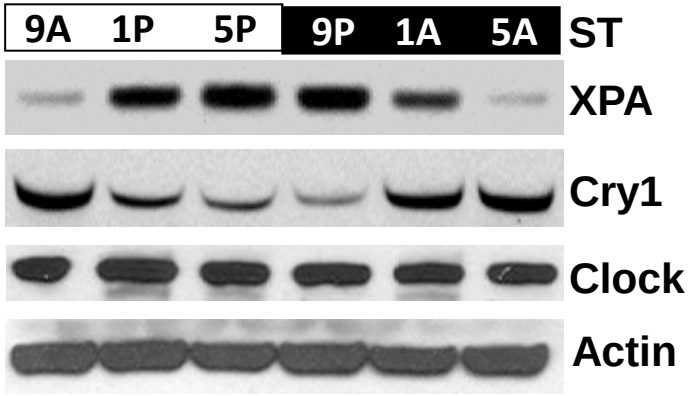

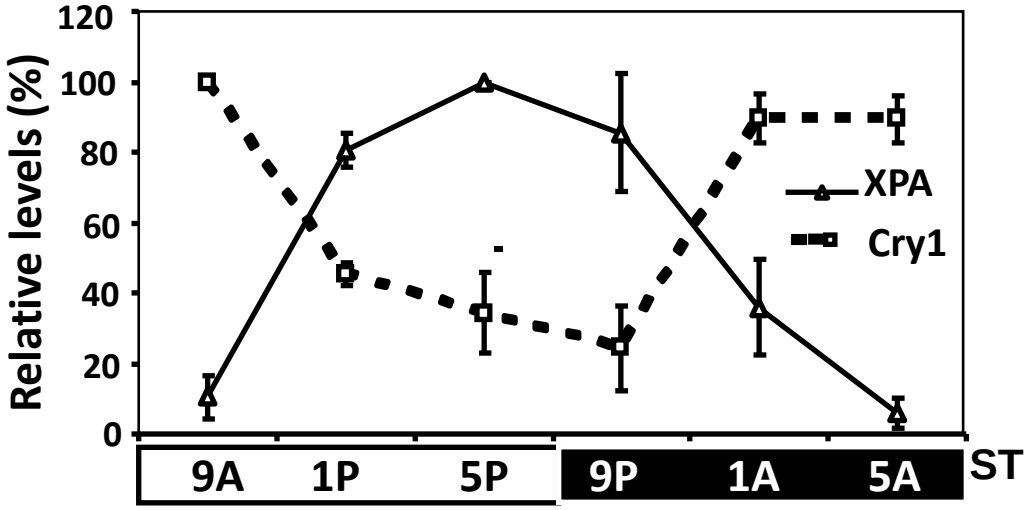

Circadian Rhythmicity of Excision Repair Rate in Mouse Epidermis

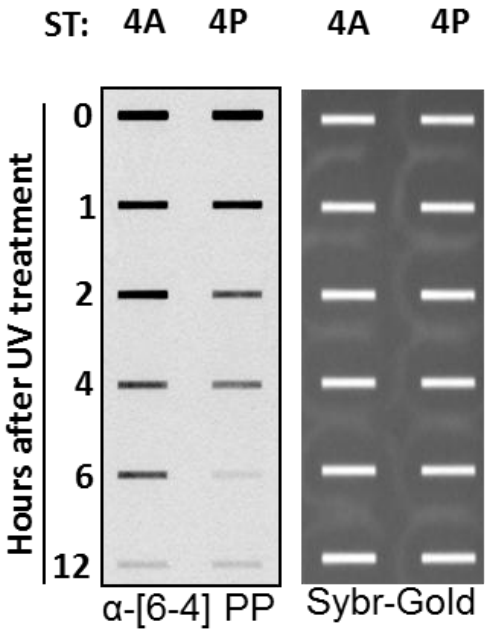

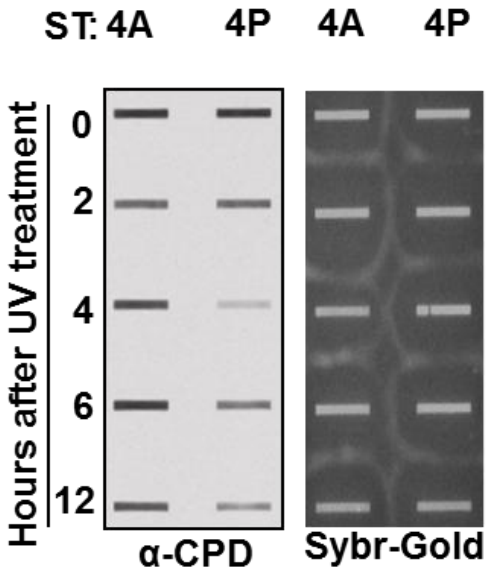

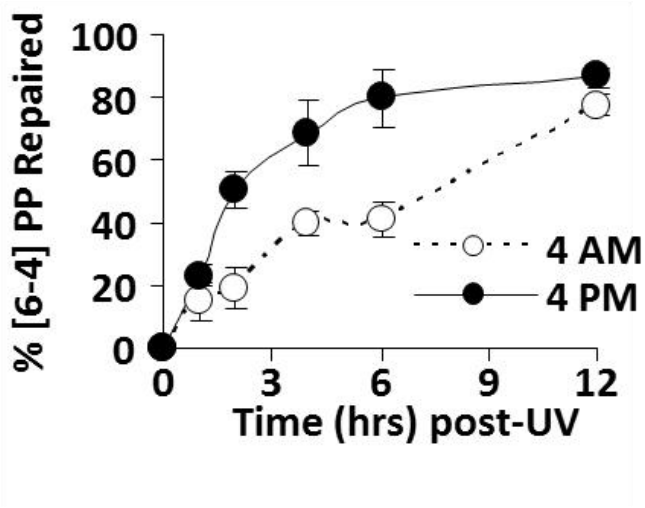

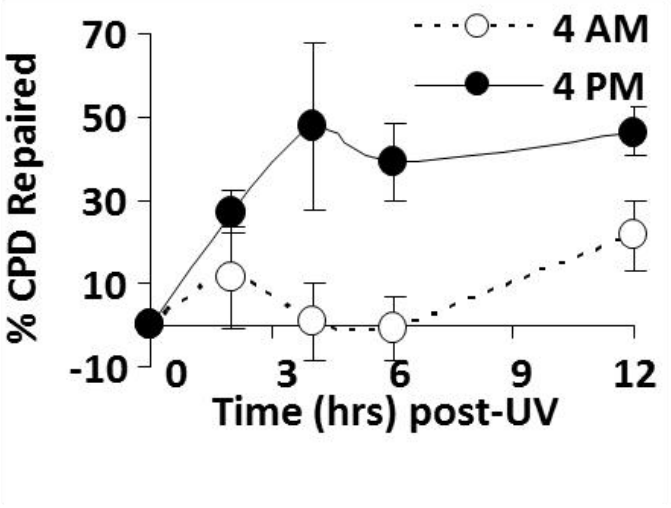

Circadian Rhythmicity of DNA Replication in Mouse

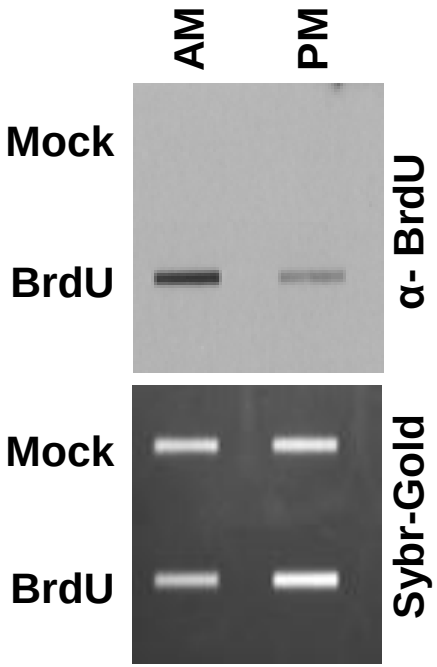

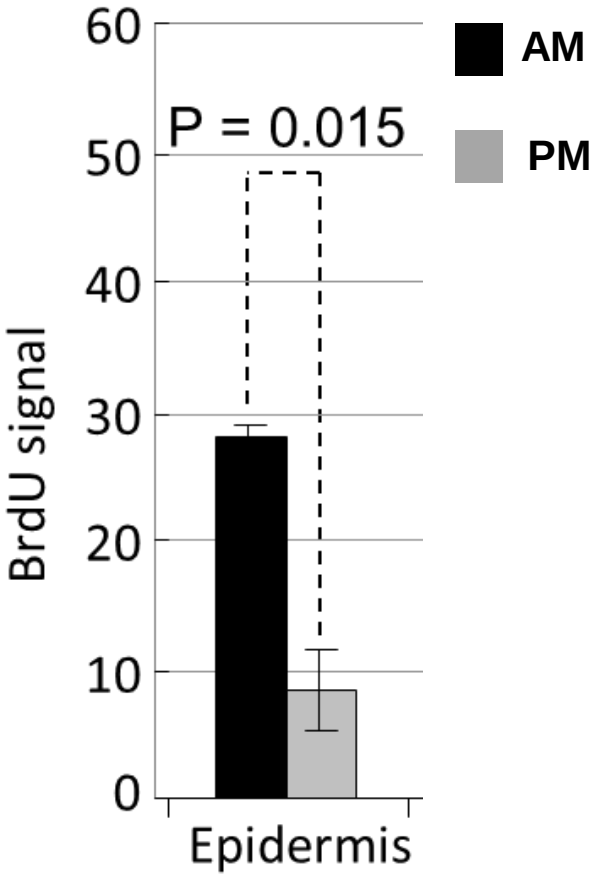

Does Skin Cancer Incidence Depend on Time of Day?

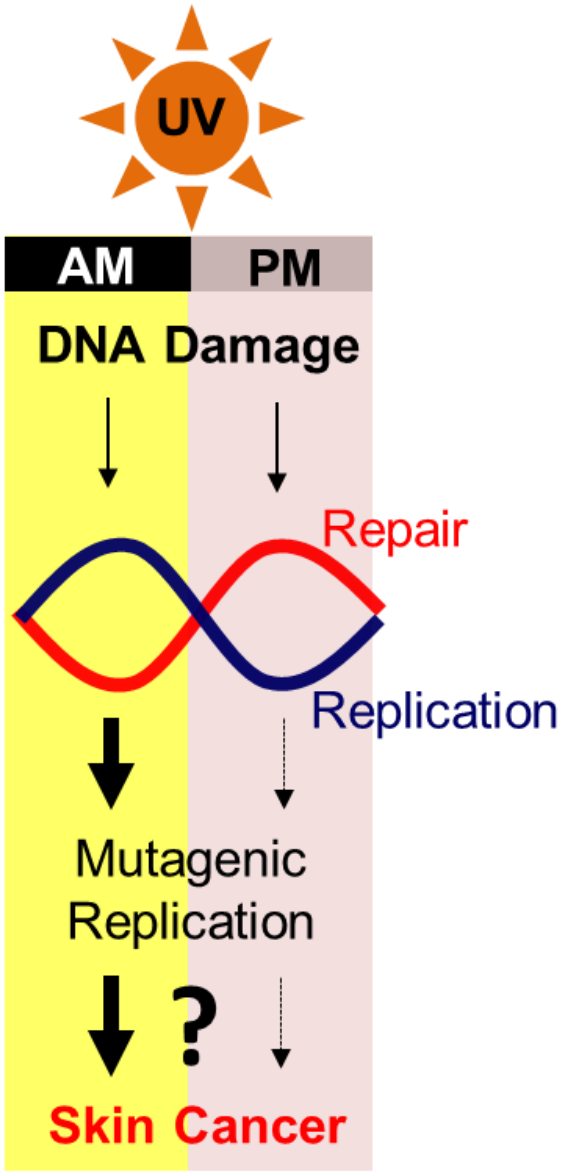

Skin Carcinogenesis Protocol

- Irradiate Mice with UVB 3 times a week for 25 weeks:
  - AM Group – 4 AM (ZT 21),
  - PM Group – 4 PM (ZT 09)
  - Control Group- No Treatment
- Examine skin daily for 25 weeks
- Analyze skin lesions histopathologically

Effect of Time of Day on UV- Skin Carcinogenesis (Visual Diagnosis) in Mouse

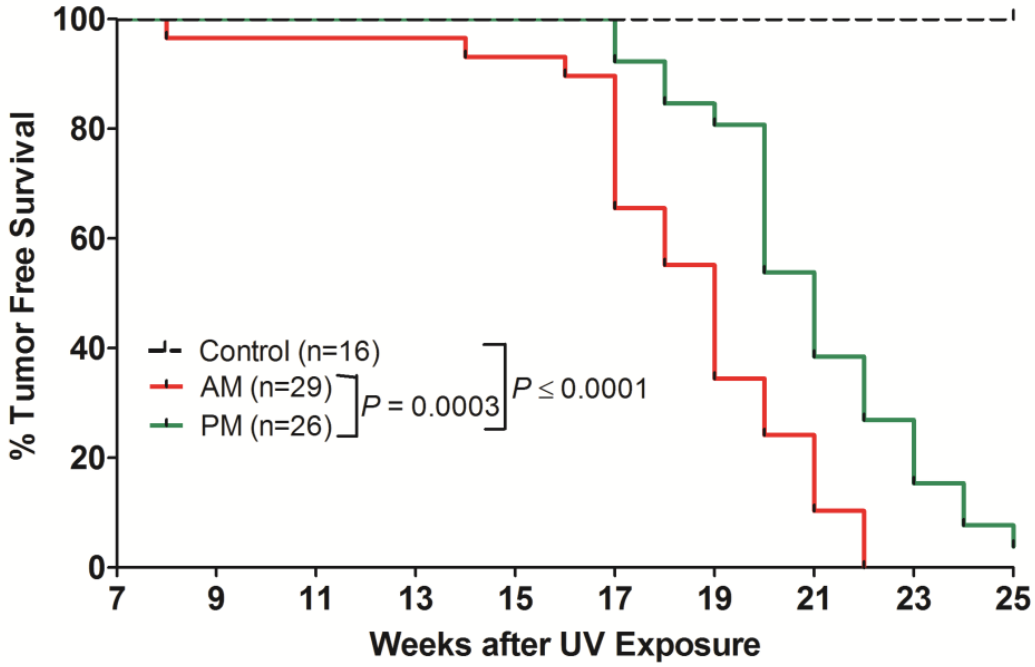

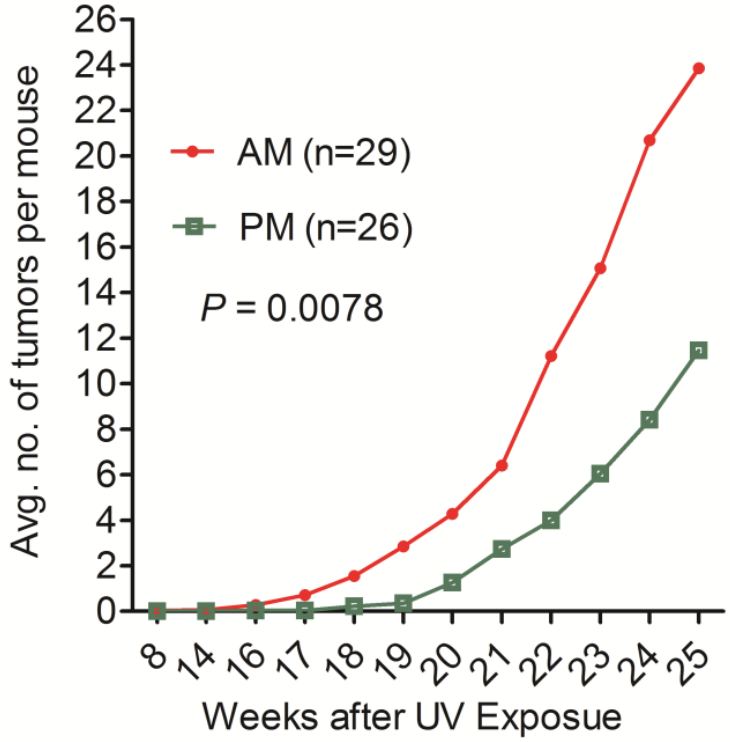

Effect of Time of Day on UV- Skin Carcinogenesis (Histopathological Examination) in Mouse

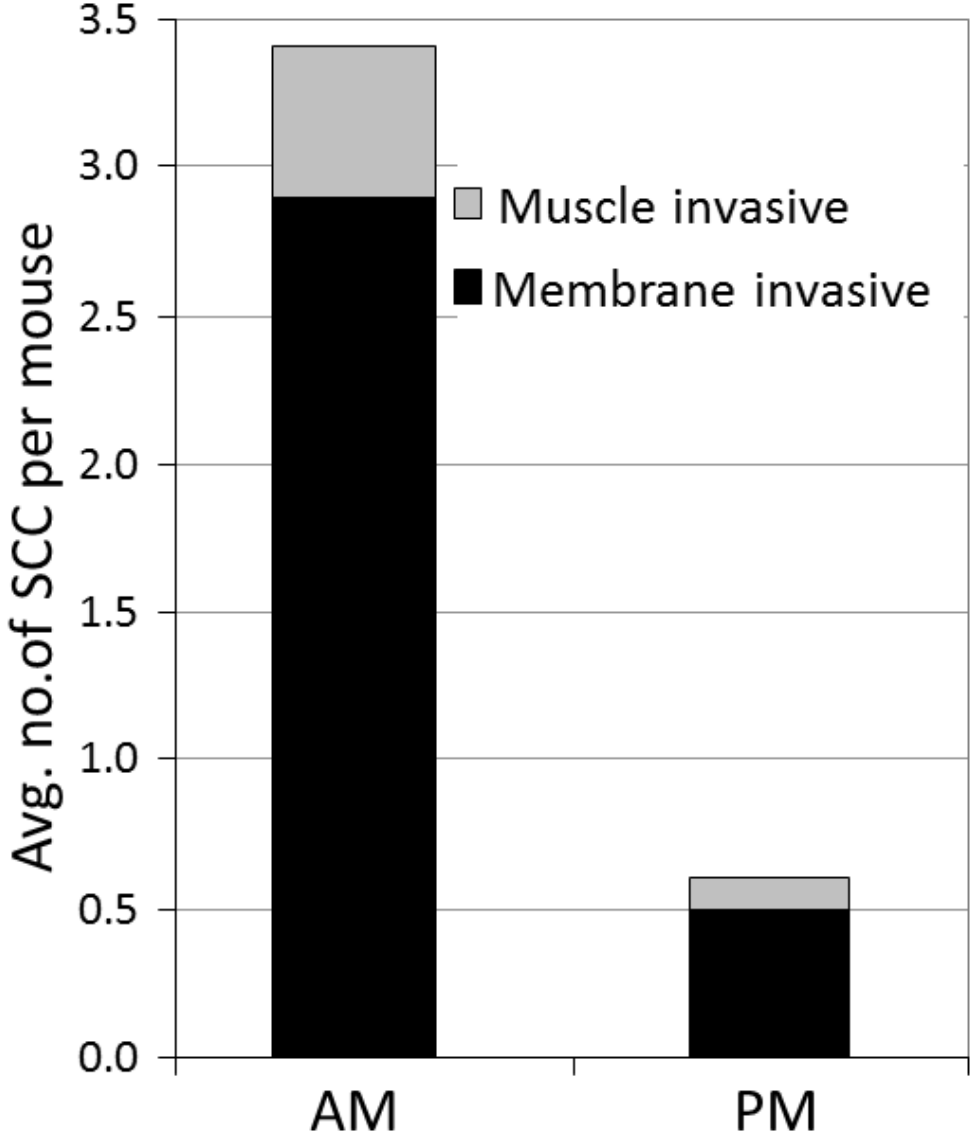

Conclusion: Model for the Role of Circadian Clock in UV-induced Skin Carcinogenesis

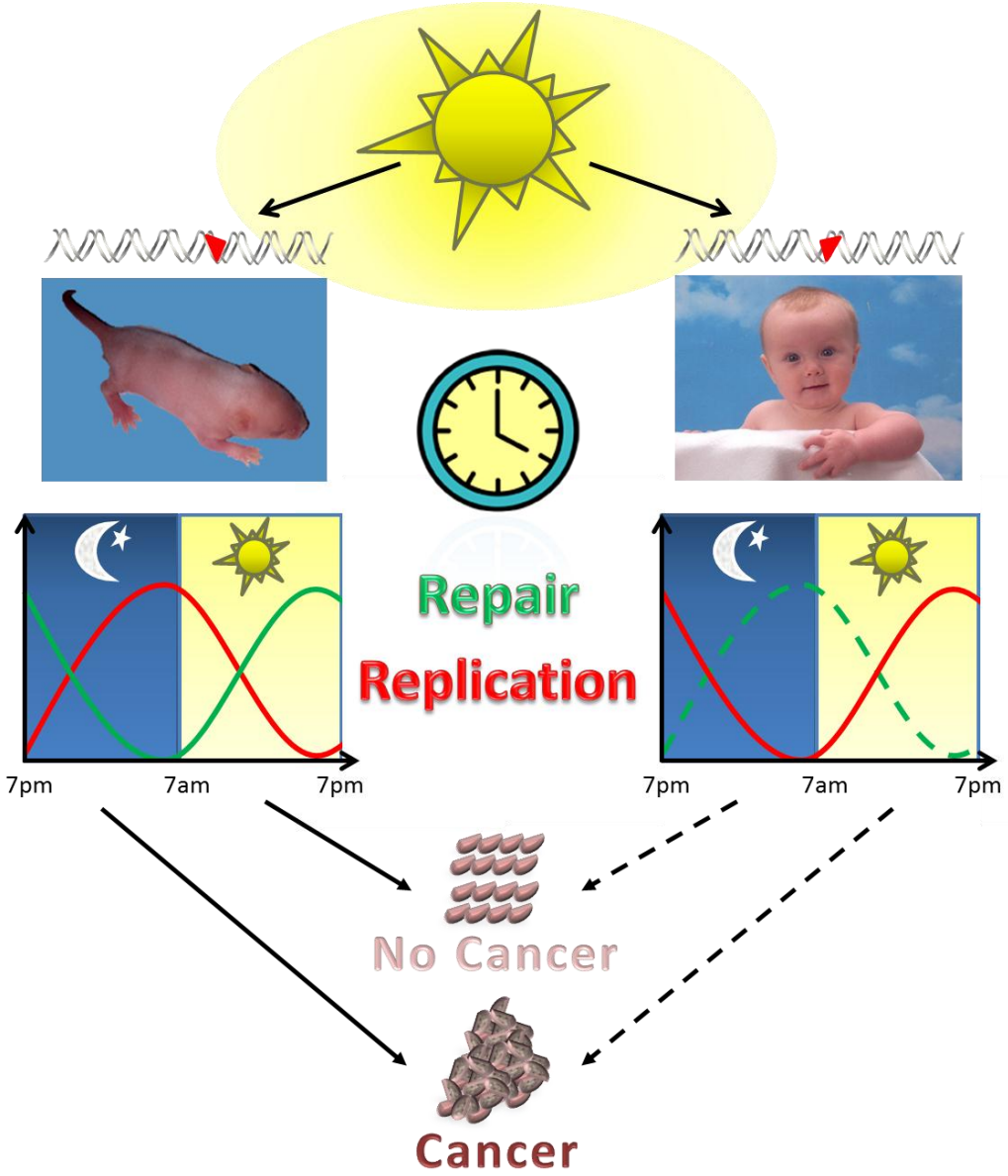

Acknowledgment

Dr. Aziz Sancar

Sancar Lab

Dr. Christopher P. Selby
Dr. Laura Lindsey-Boltz
Dr. Michael Kemp
Dr. Joyce Reardon
Dr. Christopher Capp
Dr. Rui Ye
Other Members of the Lab

Dr. Marila Cordeiro-Stone -UNC-CH
Dr. William K. Kaufmann -UNC-CH
Dr. Robert Smart -NC State

Questions?

November 15, 2011 | vol. 108 | no. 46 | 18567–18854

PNAS

Proceedings of the National Academy of Sciences of the United States of America www.pnas.org

In This Issue

Time of UV exposure might influence skin cancer onset

Exposure to UV radiation triggers DNA lesions that can lead to skin cancer, the most common type of cancer in the United States. Previous studies in mice have shown that levels of a protein called XPA, involved in repairing UV-induced DNA lesions, waxes and wanes with the time of day, peaking between 4–6 PM and dipping between 4–6 AM in tune with the circadian clock. Shobhan Gaddameedhi et al. (pp. 18790–18795) found that the protein's level and activity in mouse skin cells are at their lowest at 4 AM and their highest at 4 PM. The authors exposed two groups of mice to UV radiation—one at 4 AM and the other at 4 PM—and monitored the onset of skin cancer. Mice irradiated when the repair activity was at its lowest developed tumors much faster and at five-fold higher frequency compared with mice exposed to UV when the protein's repair function was at full throttle. When the authors repeated the experiment in a strain of mice lacking two key components of the circadian clock, the time of UV exposure tracked neither the protein's repair activity nor the onset of skin cancer, suggesting that circadian control of the XPA protein might influence skin cancer rates. Because mouse and human circadian clocks are similar, the time of UV exposure might likewise determine its cancer-causing potential in people, according to the authors. — P.N.

Image courtesy of Marian Miller (University of Cincinnati, Cincinnati, OH). Upper left quadrant: *Hourtide* by Edward Henry Potthast, 1920; Lower left quadrant: *Sleeping Woman* by Felix Valloton, 1899.

Circadian control of skin cancer.

Gaddameedhi S *et al* (**2011**) PNAS 108:18790-18795